Determining Generalized Parton Distributions

via Deep Exclusive Meson Production at SoLID

Zafar Ahmed
University of Regina

Outline

- Introduction to QCD and GPDs
- Properties of GPDs
- GPDs in DEMP
- Physical Content of GPDs
- Solenoid Large Intensity Detector (SoLID)
- Proposed results of Jefferson PAC approved experiment E12-10-006B

QCD and Standard Model

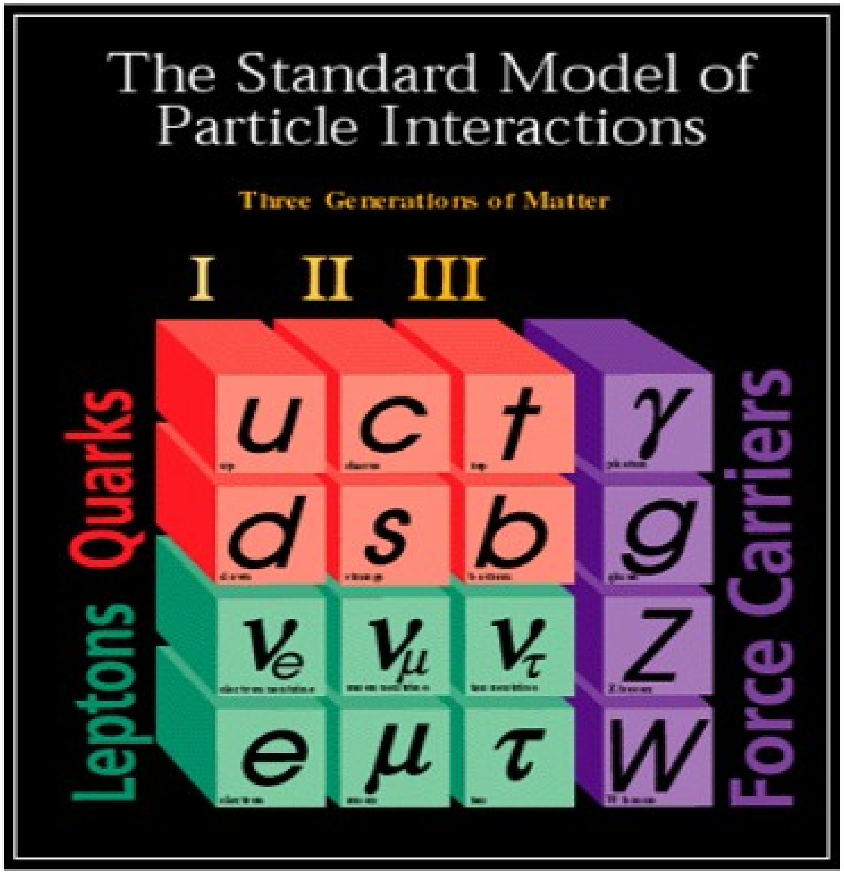

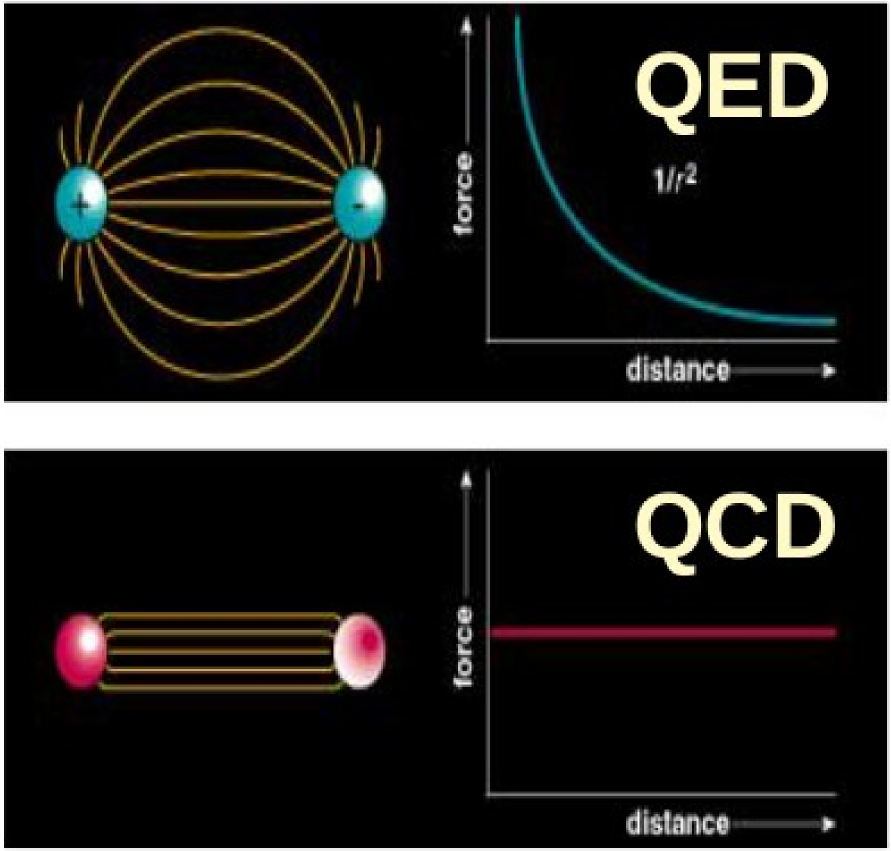

- Quarks are fractionally charged and interact via the electromagnetic (QED) and strong (QCD) interactions.
- Unlike the photons of QED, the gluons of QCD carry color charge and interact strongly, leading to the confinement of quarks inside hadrons.

QCD at High and Low Q^2

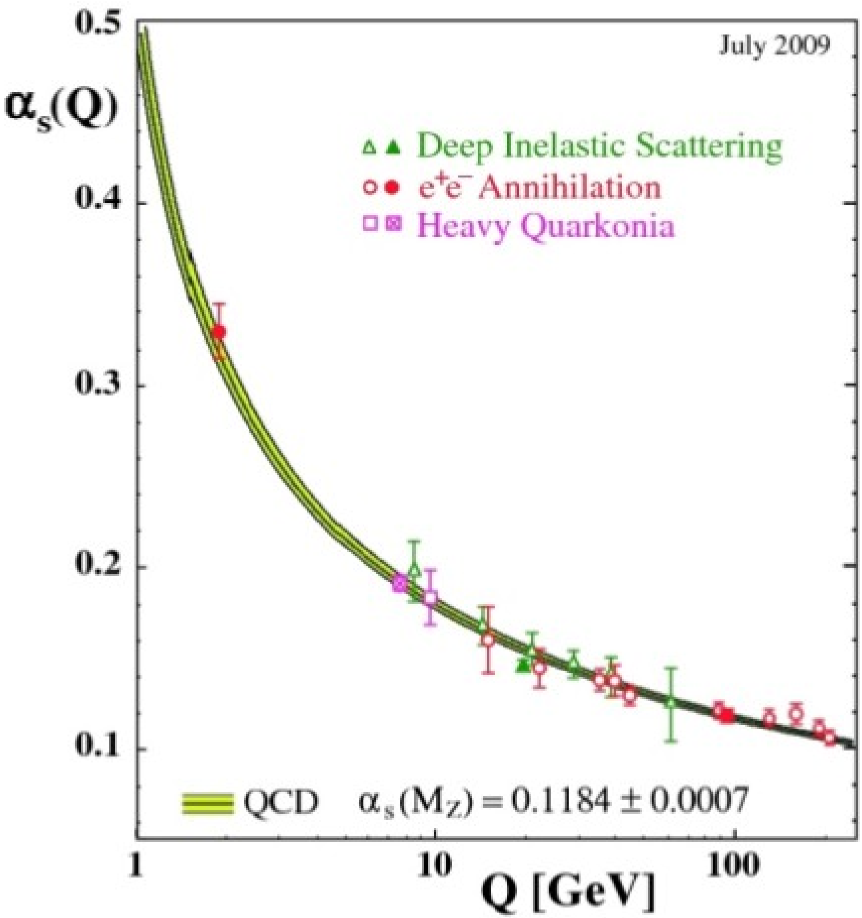

Short Distance Interaction:

- Short distance quark-quark interaction is feeble.
  - Quarks inside protons behave as if they are nearly unbound.
  - Asymptotic Freedom.
- perturbative QCD (pQCD).

Long Distance Interaction:

- Quarks strongly bound within hadrons.
  - Color confinement (strong QCD).
- QCD calculations extremely difficult.
- **QCD-based models often used, but experimental data needed to validate approaches used.**
- **Studies are at the interface of particle and nuclear physics since the problems often require a "many body" approach.**

Need for GPDs

- Description of hadrons in terms of partons (Quarks and Gluons)
- Description of nucleon mass and spin in terms of partons
- We are looking for three dimensional picture of proton with momentum and space distribution of partons in proton
- In order to probe quarks in proton we need high Qsq
- With high Qsq value the virtual photon sees the proton as a disk rather than a sphere
- From Factors provide two dimensional spatial distribution of partons
- Parton distribution functions (PDF) gives longitudinal momentum information
- We need distributions functions of partons which correlate longitudinal momentum and transverse spatial distributions of partons in proton

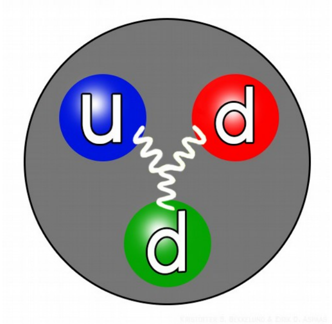

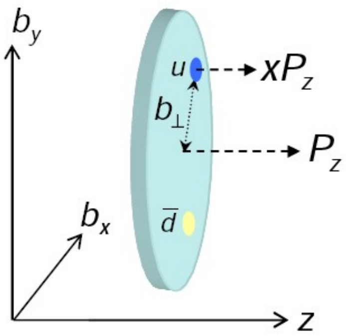

Useful Kinematic Variables of Inelastic Scattering

- $x = (x_0 , x_1 ,x_2 ,x_3)$
- Light cone coordinates: $x^+ = (x_0 + x_3) / \sqrt{2}$, $x^- = (x_0 - x_3) / \sqrt{2}$, $x^T = (x^1 , x^2)$
- $x = (x^+ , x^- , x^T)$

- GPDs are function of x, -t and ξ.
- P_n, P_p Neutron(initial) and Recoil Proton(final) nucleon momentum
- $P_e , P_{e'}$ Initial and final electron momentum
- k struck quark momentum
- $q = (P_{e'} - P_e)$ virtual photon momentum
- $P = P_n + P_p$
- $\Delta = P_n - P_p$
- $Q^2 = -(P_e – P_{e'})^2$
- $x = k^+ / P^+$
- $\xi = \Delta^+ / P^+$
- $-t = \Delta^2$
- $x_B = Q^2 / (2P_n.q)$

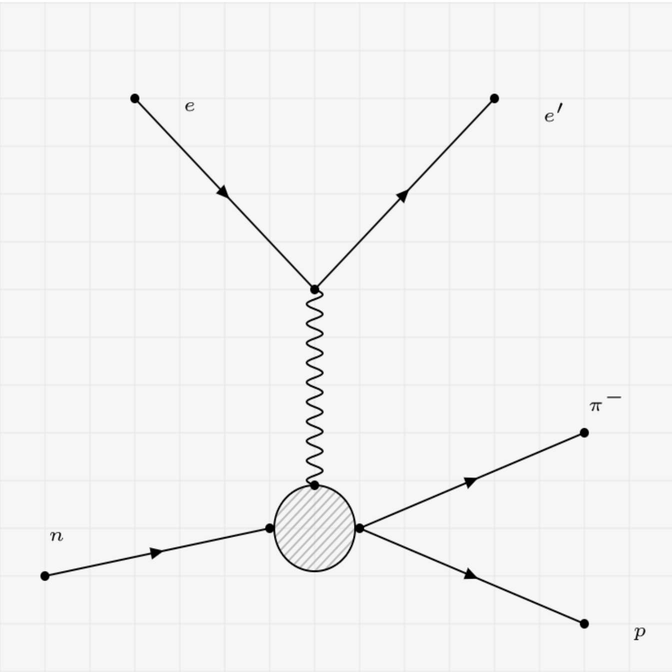

GPD Definition

- Electron proton scattering cross section: $d\sigma \sim L_{\mu\nu} W^{\mu\nu}$
- All the information about proton is in hadronic tensor $W^{\mu\nu}$
- Elastic scattering of electron from an extended proton with electromagnetic interaction.

$$\bar{u}(p_2)(\Gamma_\mu)u(p_1) = \bar{u}(p_2)\left(\gamma_\mu F_1(q^2) + i\frac{1}{2M_0}F_2(q^2)q^\nu\sigma_{\mu\nu}\right)u(p_1)$$

- Deep inelastic electron proton scattering with strong interaction. Q^2 is high so virtual photon interact with one quark in proton. k is momentum struck quark.
- Hadronic tensor with QCD parton model [1]:

$$2MW^{\mu\nu} = \sum_q e_q^2 \int d^4p \quad \delta((p+q)^2 - m^2) \quad \theta(p^0+q^0-m) \times Tr[\Phi(p,P,S)\gamma^\mu(\not{p}+\not{q}+m)\gamma^\nu + \bar{\Phi}(p,P,S)\gamma^\nu(\not{p}+\not{q}+m)\gamma^\mu]$$

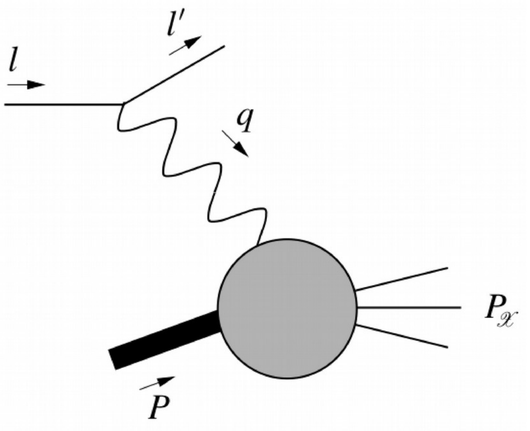

- Φ is quark-quark correlation function:

$$\Phi_{ji} = \frac{1}{(2\pi)^4}\int d^4z e^{-ip.z}\langle P|\bar{\psi}_i(z)\psi_i(0)|P\rangle$$

- Definition equation of GPD(at leading twist, twist 2):

$$\bar{P}^+\int d\bar{p}^- d^2\bar{p}_\perp Tr(\Phi\gamma^+)\,|_{\bar{p}^+=x\bar{P}^+} = \bar{\psi}(P^f)\left[\gamma^+ H(x,\xi,t) + \frac{i\sigma^{+i}\Delta_i}{2M_p}E(x,\xi,t)\right]\psi(P)$$

$$\bar{P}^+\int d\bar{p}^- d^2\bar{p}_\perp Tr(\Phi\gamma^+\gamma_5)\,|_{\bar{p}^+=x\bar{P}^+} = \bar{\psi}(P^f)\left[\gamma^+\gamma_5\tilde{H}(x,\xi,t) + \frac{\gamma_5\Delta_i}{2M_p}\tilde{E}(x,\xi,t)\right]\psi(P)$$

Few Comments about GPD

- Four more transversity GPDs: H_T, E_T, $\tilde{E}_T$ and $\tilde{H}_T$
- For each quark flavor there are Eight GPDs.
- GPDs encode non-perturbative dynamics of partons in hadrons [2]
- GPDs give momentum correlation of quarks in hadron [2]
- With Fourier transform we can access longitudinal momentum fraction of quarks and position of quarks in the transverse plane [3]
- GPDs reflect the structure of nucleon independent of the reaction[5]
- In DEMP process higher twist contribution to GPDs is not negligible at amplitude level but it is negligible in asymmetry
- On a proton target, the GPD *H* describes the distribution of unpolarized quarks in an unpolarized nucleon[15]
- GPD $\tilde{H}$, which describes the distribution of (longitudinally) polarized quarks in a (longitudinally) polarized nucleon[15]
- GPD *E* is related to orbital angular momentum of quarks

GPDs in DEMP

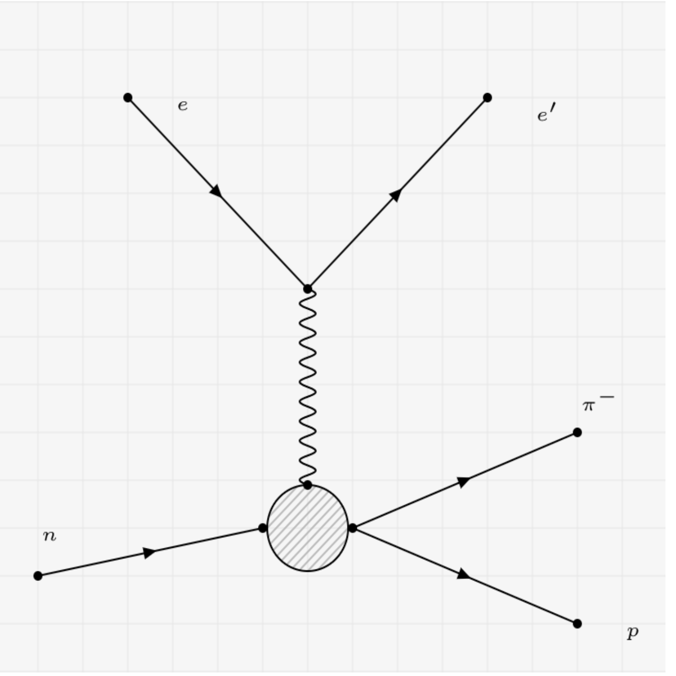

- Deep exclusive meson electroproduction:
- For high enough Q^2 we can assume:
- One photon exchange
- Virtual photon interacts with one quark
- Quark only interact with virtual photon

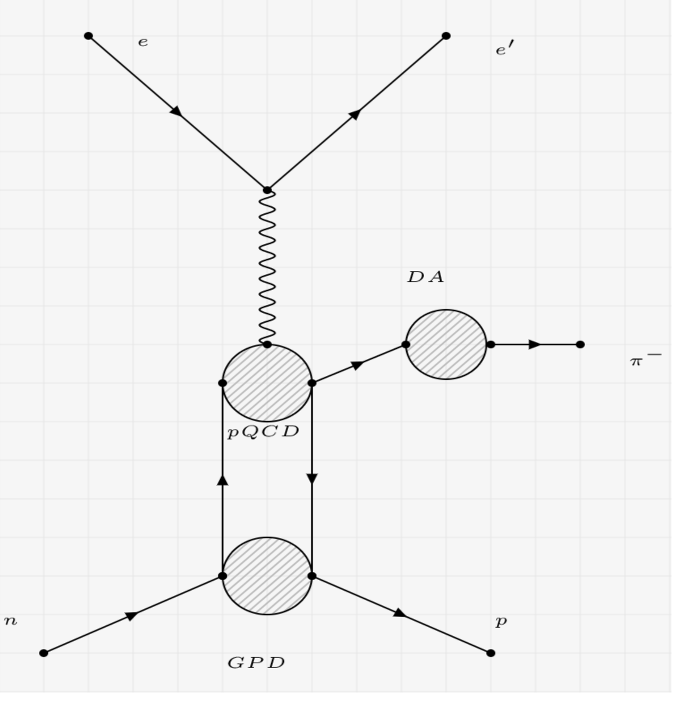

- Hard Exclusive Meson Electroproduction first shown to be factorizable by Collins, Frankfurt & Strikman [PRD 56(1997)2982].
- Factorization int pQCD and GPD part of hadronic tensor is possible when virtual photon has longitudinal polarization.
- Conditions for factorization: High Q^2 , high W and $|t| / Q^2 << 1$
- Amplitudes for transversely polarized photons is suppressed by 1/Q

GPD Properties

- In forward limit, $\xi \rightarrow 0$ and for high Q^2 we have $x \rightarrow x_B$, H and $\tilde{H}$ reduces PDFs of DIS [4]

$$H^q(x,0,0) = \begin{cases} q(x_B), & x_B > 0 \\ -q(-x_B), & x_B < 0 \end{cases}$$

$$\tilde{H}^q(x,0,0) = \begin{cases} \Delta q(x_B), & x_B > 0 \\ \Delta \bar{q}(-x_B), & x_B < 0 \end{cases}$$

- where $q(x_B)$, $-\bar{q}(x_B)$, $\Delta q(x_B)$ and $-\Delta\bar{q}(x_B)$ are quark (antiquark) density and helicity distributions respectively. No corresponding relations exist for the functions E and $\tilde{E}$.

- The relation between angular momentum of quarks in nucleon and second Mellin moment of GPDs H and E is give by sum rule [5]

$$\int_{-1}^{1} dx \quad x \quad (H^q(x,\xi) + E^q(x,\xi)) = 2J^q$$

- where J^q is the fraction of nucleon angular momentum carried by a quark flavor q

GPD Properties. Form Factor

- First Mellin moments of GPDs are related to elastic form factors of the nucleon [5]

$$\int_{-1}^{1} dx \quad H^q(x,\xi,t) = F_1^q(t) \qquad \int_{-1}^{1} dx \quad \tilde{H}^q(x,\xi,t) = g_A^q(t)$$

$$\int_{-1}^{1} dx \quad E^q(x,\xi,t) = F_2^q(t) \qquad \int_{-1}^{1} dx \quad \tilde{E}^q(x,\xi,t) = h_A^q(t)$$

- where F_1^q, F_2^q , g_A^q and h_A^q are Dirac, Pauli, axial and pseudoscaler and form factors. Equation between quarks form factors and proton form factors are given by

$$F^{u/p} = 2F_1^p + F^n + F_1^s \qquad g_A^u = \frac{1}{2}g_A + \frac{1}{2}h_A^0$$

$$F^{d/p} = 2F_1^n + F^p + F_1^s \qquad g_A^d = -\frac{1}{2}g_A + \frac{1}{2}g_A$$

- $F^{u/p}$ is up quark form factor in proton.

DEMP Cross Section

- Deep inelastic scattering of electron and nuclec
- Neutron splits in π and recoil proton
- Scattering Cross section:[6] $d\sigma = d\sigma_{UU} + d\sigma_{UT}$

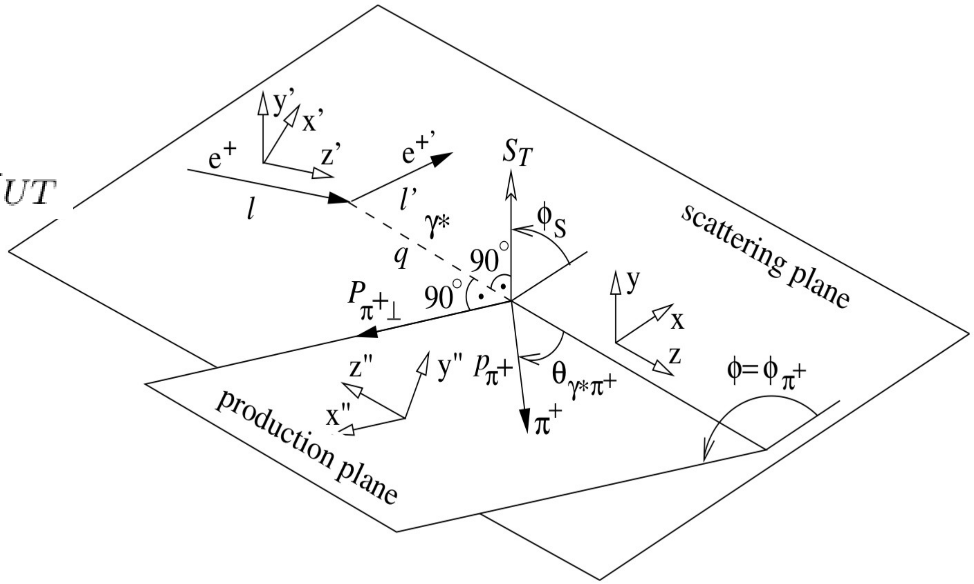

Photo taken from [6]

$$d\sigma_{UU} = \frac{1}{2}(\sigma_{++}^{++} + \sigma_{++}^{--}) + \varepsilon\sigma_{00}^{++} - \varepsilon\cos(2\phi)\,\mathrm{Re}\,\sigma_{+-}^{++} - \sqrt{\varepsilon(1+\varepsilon)}\cos\phi\;\mathrm{Re}\,(\sigma_{+0}^{++} + \sigma_{+0}^{--})$$

$$d\sigma_{UU} = \frac{d\sigma_{\mathrm{T}}}{dt} + \epsilon\frac{d\sigma_{\mathrm{L}}}{dt} + \epsilon\cos 2\phi\frac{d\sigma_{\mathrm{TT}}}{dt} + \sqrt{2\epsilon(\epsilon+1)}\cos\phi\frac{d\sigma_{\mathrm{LT}}}{dt}$$

$$d\sigma_{UT} = -\frac{P_T}{\sqrt{1-\sin^2\theta\sin^2\phi_S}}\sum_{k=1}^{6}\sin(\mu\phi+\lambda\phi_S)_k\;\Sigma_k,$$

k	$\sin(\mu\phi+\lambda\phi_S)_k$ azimuthal modulation	Σ_k polarised photoabsorption cross section/interference term
1	$\sin(\phi-\phi_S)$	$\cos\theta\,\mathrm{Im}\,(\sigma_{++}^{+-} + \varepsilon\sigma_{00}^{+-}) + \frac{1}{2}\sin\theta\sqrt{\varepsilon(1+\varepsilon)}\,\mathrm{Im}\,(\sigma_{+0}^{++} - \sigma_{+0}^{--})$
2	$\sin(\phi+\phi_S)$	$\frac{1}{2}\cos\theta\,\varepsilon\,\mathrm{Im}\,\sigma_{+-}^{+-} + \frac{1}{2}\sin\theta\sqrt{\varepsilon(1+\varepsilon)}\,\mathrm{Im}\,(\sigma_{+0}^{++} - \sigma_{+0}^{--})$
3	$\sin\phi_S$	$\cos\theta\sqrt{\varepsilon(1+\varepsilon)}\,\mathrm{Im}\,\sigma_{+0}^{+-}$
4	$\sin(2\phi-\phi_S)$	$\cos\theta\sqrt{\varepsilon(1+\varepsilon)}\,\mathrm{Im}\,\sigma_{+0}^{-+} + \frac{1}{2}\sin\theta\,\varepsilon\,\mathrm{Im}\,\sigma_{+-}^{++}$
5	$\sin(3\phi-\phi_S)$	$\frac{1}{2}\cos\theta\,\varepsilon\,\mathrm{Im}\,\sigma_{+-}^{-+}$
6	$\sin(2\phi+\phi_S)$	$\frac{1}{2}\sin\theta\,\varepsilon\,\mathrm{Im}\,\sigma_{+-}^{++}$

- Subscript of **σ** is polarization of nucleon and superscript is polarization of photon

Dominant Amplitude in Azimuthal Asymmetries

- Azimuthal asymmetry is defined as [6]

$$A(\phi, \phi_S) = \frac{1}{|P_T|} \frac{d\sigma(\phi, \phi_S) - d\sigma(\phi, \phi_S + \pi)}{d\sigma(\phi, \phi_S) + d\sigma(\phi, \phi_S + \pi)} = \frac{d\sigma_{UT}(\phi, \phi_S)}{d\sigma_{UU}(\phi)}$$

$$A(\phi, \phi_S) = -\frac{\sum_{k=1}^{6} \sin(\mu\phi + \lambda\phi_S)_k \Sigma_k}{d\sigma_{UU}(\phi)} = -\sum_{k=1}^{6} A_{UT}^{\sin(\mu\phi+\lambda\phi_S)_k} \sin(\mu\phi + \lambda\phi_S)_k$$

$$\begin{aligned} A(\phi, \phi_S) = &- A_{UT}^{\sin(\phi-\phi_S)} \sin(\phi - \phi_S) - A_{UT}^{\sin(\phi+\phi_S)} \sin(\phi + \phi_S) - A_{UT}^{\sin\phi_S} \sin\phi_S \\ &- A_{UT}^{\sin(2\phi-\phi_S)} \sin(2\phi - \phi_S) - A_{UT}^{\sin(3\phi-\phi_S)} \sin(3\phi - \phi_S) \\ &- A_{UT}^{\sin(2\phi+\phi_S)} \sin(2\phi + \phi_S). \end{aligned}$$

- Each of the six asymmetry has dominating amplitude given by:[7]

observable	dominant interf. term	amplitudes	low t' behavior
$A_{UT}^{\sin(\phi-\phi_s)}$	LL	$\mathrm{Im}[\mathcal{M}^*_{0-,0+}\mathcal{M}_{0+,0+}]$	$\propto \sqrt{-t'}$
$A_{UT}^{\sin(\phi_s)}$	LT	$\mathrm{Im}[\mathcal{M}^*_{0-,++}\mathcal{M}_{0+,0+}]$	const.
$A_{UT}^{\sin(2\phi-\phi_s)}$	LT	$\mathrm{Im}[\mathcal{M}^*_{0-,-+}\mathcal{M}_{0+,0+}]$ 1)	$\propto t'$
$A_{UT}^{\sin(\phi+\phi_s)}$	TT	$\mathrm{Im}[\mathcal{M}^*_{0-,++}\mathcal{M}_{0+,++}]$	$\propto \sqrt{-t'}$
$A_{UT}^{\sin(2\phi+\phi_s)}$	TT	$\propto \sin\theta_\gamma$	$\propto t'$
$A_{UT}^{\sin(3\phi-\phi_s)}$	TT	$\mathrm{Im}[\mathcal{M}^*_{0-,-+}\mathcal{M}_{0+,-+}]$	$\propto (-t')^{(3/2)}$
$A_{UL}^{\sin(\phi)}$	LT	$\mathrm{Im}[\mathcal{M}^*_{0-,++}\mathcal{M}_{0-,0+}]$	$\propto \sqrt{-t'}$

- Where $M_{(mi)(nj)} = \sigma_{mn}^{ij}$

Amplitudes $M_{mi,nj}$ Relation to GPDs

- Matrix elements of Pion π^+ production scattering amplitude:[8]

$$\mathcal{M}_{0+,0+} = \frac{e_0}{Q}\sqrt{1-\xi^2}\int_{-1}^{1} dx \mathcal{H}_{0+0+}\left[\widetilde{H} - \frac{\xi^2}{1-\xi^2}\widetilde{E}\right]$$
$$\mathcal{M}_{0-,0+} = \frac{e_0}{Q}\frac{\sqrt{-t'}}{2m}\xi\int_{-1}^{1} dx \mathcal{H}_{0+0+}\widetilde{E}\,,$$

- Where H_{0+0+} denotes the subprocess amplitude
- $t' = t - t_0$ where t_0 is value of t in parallel kinematics
- More relations between scattering amplitudes and GPDs are give in [9]
- Accessing GPDs via DEMP[10]

GPD	Probed by
$H(val)$	ρ^0, ϕ cross section
$H(g, sea)$	ρ^0, ϕ cross section
$E(val)$	$A_{UT}(\rho^0, \phi)$
$E(g, sea)$	-
$\tilde{H}(val)$	π^+ data
$\tilde{H}(g, sea)$	$A_{LL}(\rho^0)$
$\tilde{E}(val)$	π^+ data
$H_T, \bar{E}_T(val)$	π^+ data

DEMP → GPD

Experimentally Measure Azimuthal Asymmetry

↓

Extract Six Asymmetries

↓

Calculate Matrix Elements of Scattering Amplitudes $M_{mi,nj}$ From Asymmetries

↓

Calculate GPDs from $M_{mi,nj}$

↓

Improve the existing picture of nucleon

1) Size of asymmetries is different for different meson productions so it provides additional constraints for GDP
2) Quark content and quantum numbers of different mesons is different. It gives different combinations of GDPs in soft part of hadronic tensor. So DEMP acts as quark flavor filter

$A_{UT}\sin(\varphi - \varphi_s)$: Spin–flip GPD $\tilde{E}$ and Pion Pole

- A manifestation of spontaneously broken chiral symmetry is pion pole term in electroproduction of pion at small value of -t
- Pseudoscaler form factor is dominated by the pion pole contribution at small -t[5]

$$\lim_{t\to m_\pi^2} h_A^q(t) = \frac{1}{2}\ \tau_{qq}^3\ \frac{4g_A m_N^2}{m_\pi^2 - t}$$

- $g_A \approx 1.267$ is the nucleon isovector axial charge and τ^3 is the Pauli matrix in the flavor space.
- First Mellin moment of $\tilde{E}$ is equal to $h_A(t)$. Presence of chiral singularity in $h_A(t)$ implies that we should expect the same singularity in $\tilde{E}$ [5]

$$\lim_{t\to m_\pi^2} \widetilde{E}^q(x,\xi,t) = \frac{1}{2}\ \tau_{qq}^3\ \frac{4g_A m_N^2}{m_\pi^2 - t}\ \theta\left[\xi - |x|\right]\ \frac{1}{\xi}\ \Phi_\pi\left(\frac{x}{\xi}\right)$$

Where is Φ_π the pion distribution amplitude

$$A_{UT}^{sin(\phi-\phi_s)} \sim Im\left(M_{0-,0+}^{*} M_{0-,0+}\right) \sim \frac{Im\left(\tilde{E}^{*}\tilde{H}\right)}{|\tilde{E}|^2} \quad where \quad \tilde{E} \gg \tilde{H}$$

$A_{UT}\sin(\varphi_s)$ and $A_{UT}\sin(2\varphi - \varphi_s)$

- **$A_{UT}\sin(\varphi_s)$** shows the contribution of transversely polarized virtual photons to electroproduction of pion[11] (Jlab data [12] and Hermes data[13])

W [GeV]	Q^2 [GeV^2]	$-t'$ [GeV^2]	$d\sigma_L/dt$	Pole	$d\sigma_T/dt$	Pole
2.308	2.215	0.000	2.078 ± 0.180	2.785	1.635 ± 0.11	0.359
2.264	2.279	0.037	1.365 ± 0.125	1.692	1.395 ± 0.08	0.243
2.223	2.411	0.050	0.980 ± 0.110	1.342	1.337 ± 0.08	0.216
2.181	2.539	0.060	0.786 ± 0.114	1.105	1.304 ± 0.08	0.200
2.127	2.703	0.087	0.564 ± 0.123	0.775	1.240 ± 0.08	0.164

Table 1 of [11]

- Larger σ_T than σ_L but pion pole contribution is small
- Transversely polarized photons contribute to pion electroproduction
- One must consider dynamics different from handbag approach which only consider helicity flip GPDs
- Transversity GPD H_T dominates
- **$A_{UT}\sin(2\varphi-\varphi_s)$** modulation has additional LT interference amplitudes contributing that are not present in $\sin(\varphi_s)$.
- Different asymmetry moments provide complementary amplitude term information.

HERMES DATA[13] and GK Data Fitting[11]
Exclusive π^+ production at HERMES

- **$A_{UT}\sin(\varphi - \varphi_s)$**
- HERMES data: $\langle x_B \rangle$=0.13, $\langle Q^2 \rangle$=2.38 GeV^2, $\langle W \rangle$= 4 GeV
- Dark circles are experimental data. G. K. use (Handbag calculation)
- Dark line fit includes longitudinal and transverse photons at $Q^2 \approx 2.45$ GeV^2 and W = 3.99 GeV
- Dashed blue line includes only longitudinal photons

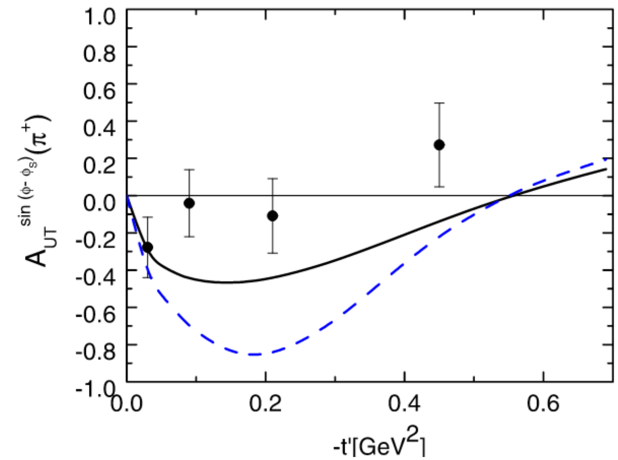

- **$A_{UT}\sin(\varphi_s)$**
- Dark line is fit including twist-3 contribution
- Dashed blue line is without twist-3 contribution at $Q^2 \approx 2.45$ GeV^2 and W = 3.99 GeV

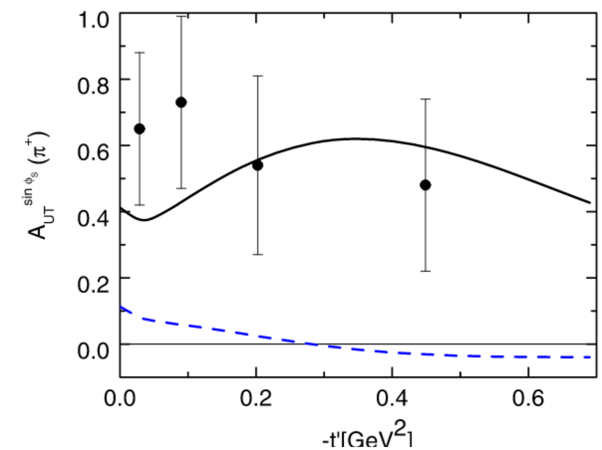

- **$A_{UT}\sin(2\varphi - \varphi_s)$**

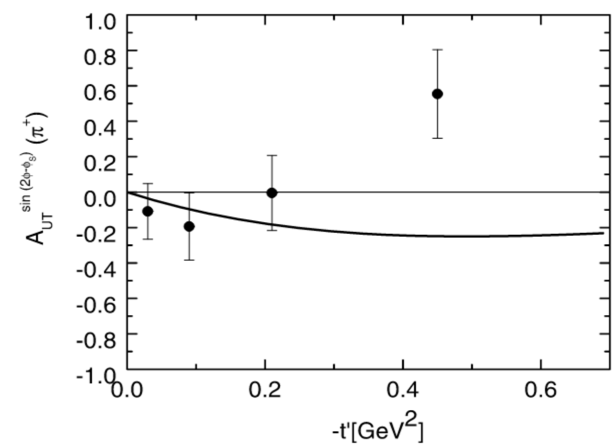

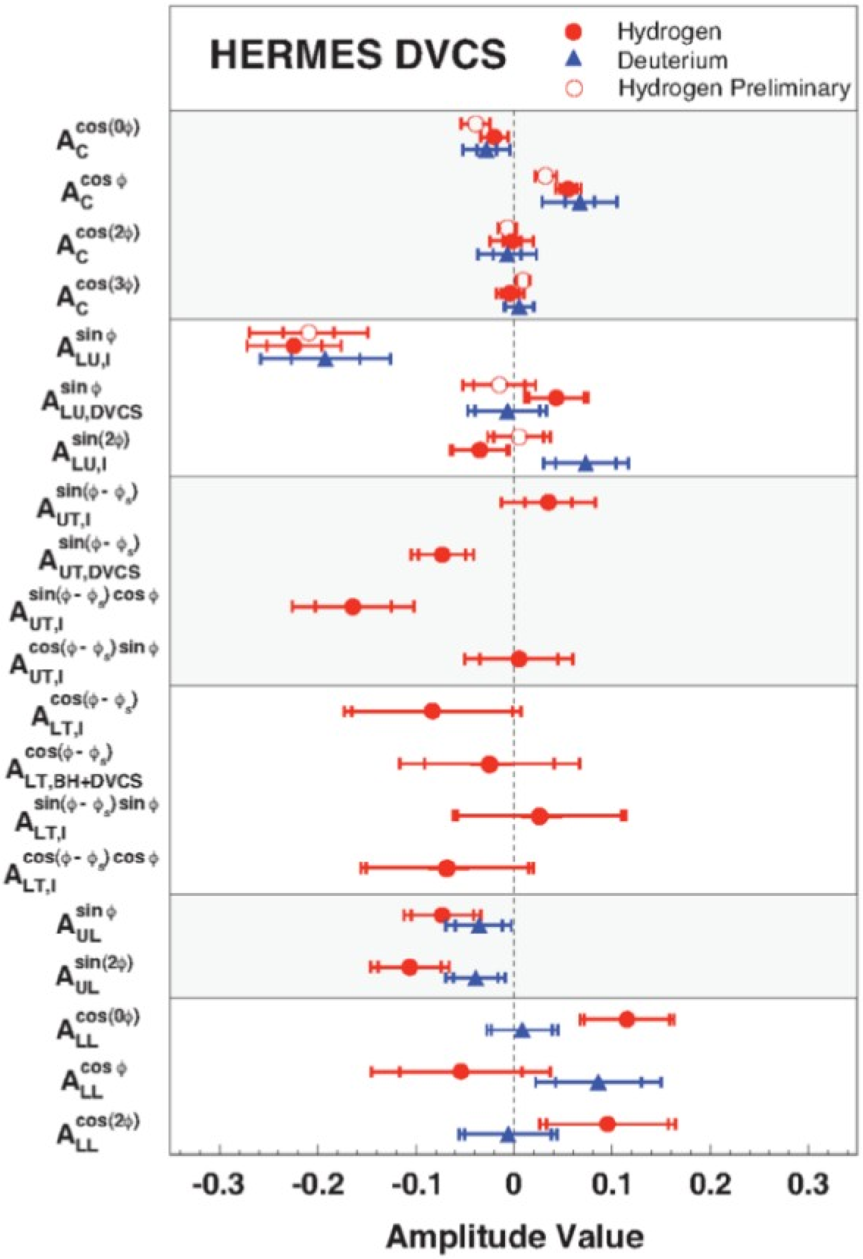

DVCS at HERMES [20]

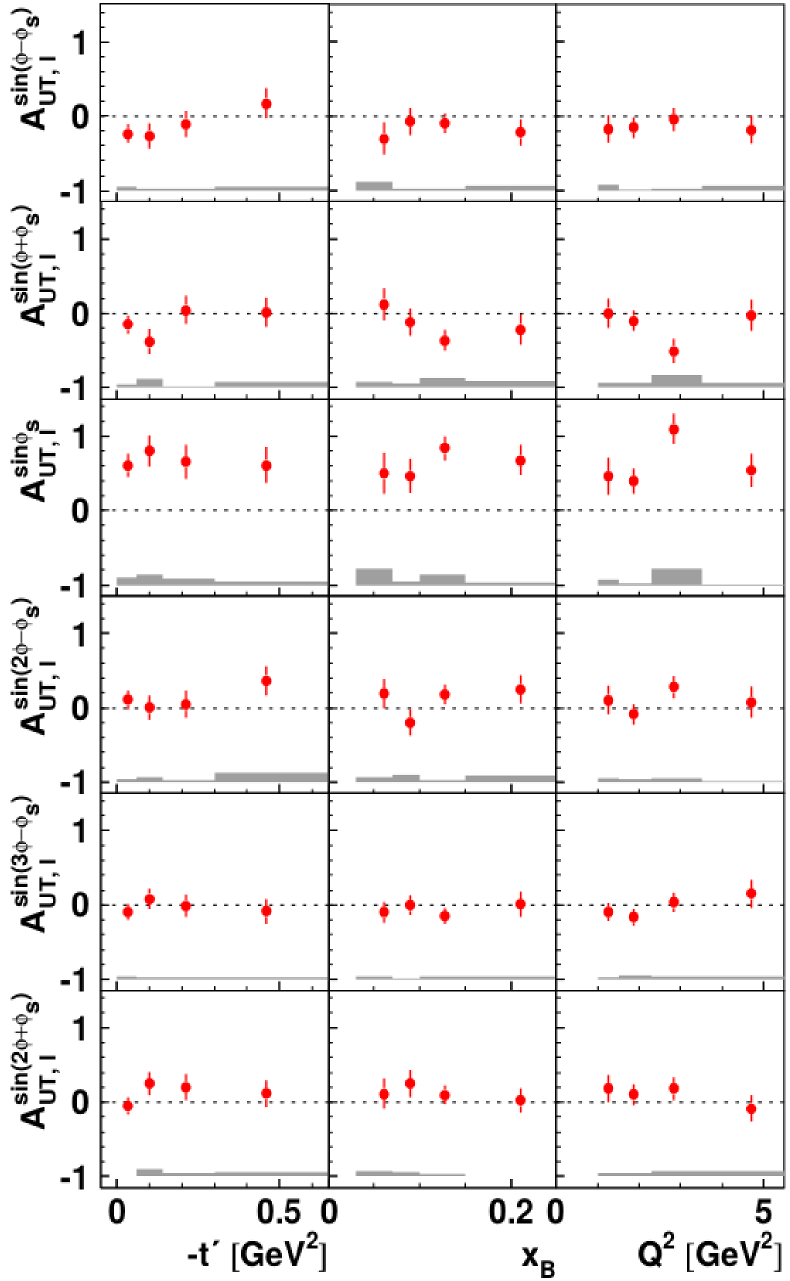

Exclusive π^+ production at HERMES

The error bars (bands) represent the statistical (systematic) uncertainties.

Exclusive ρ^0 and ω production at COMPASS [16][17]

- 160 GeV muons scatter from transversely polarized protons and deuterons

  Error bars show statistical uncertainties, while the systematic ones are represented by gray bands at the bottom and blue line is fit to data. Only E^u and E^d contribute to fit.

- For the proton these GPDs enter the amplitude as the sum $2/3\ E^u + 1/3\ E^d$
- For deuteron the effective contribution is $E^u + E^d$
- Asymmetries are small because in ρ^0 production valance quark contribution is small

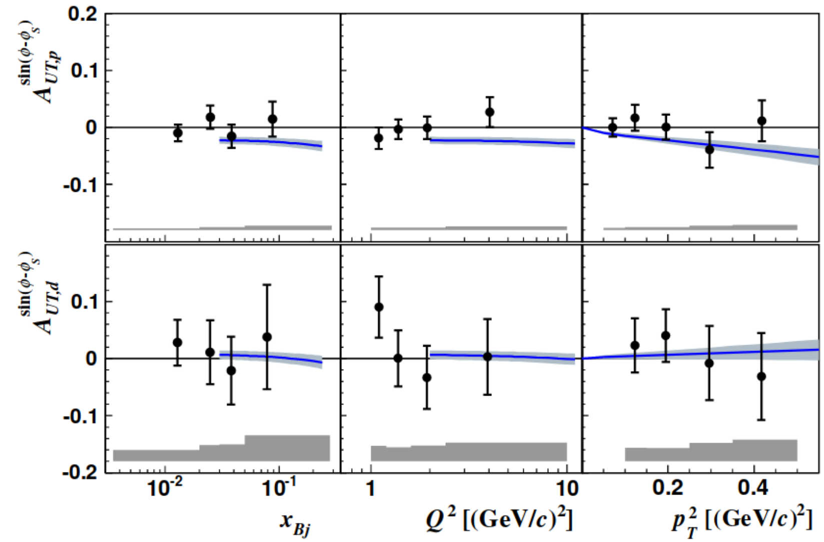

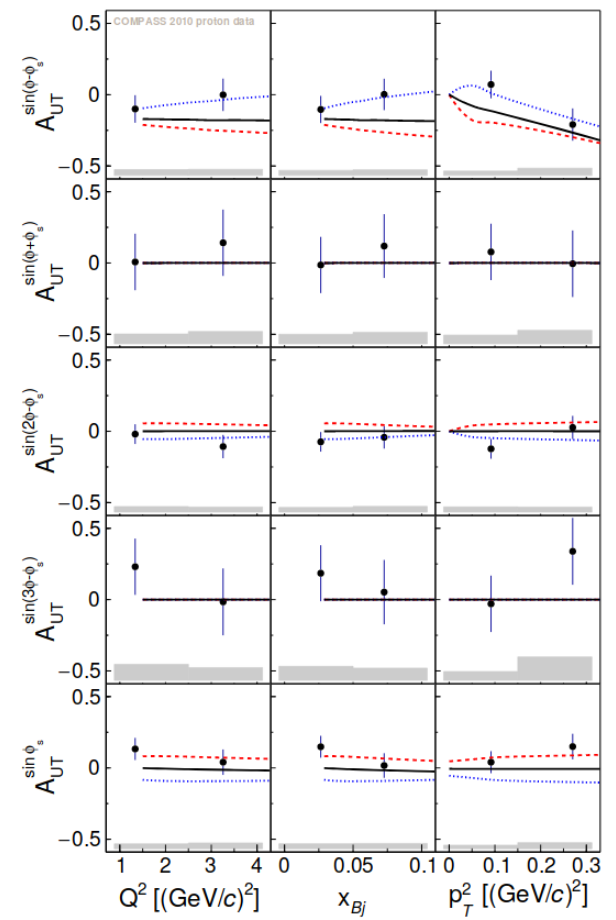

- $A_{UT}\sin(\varphi - \varphi_s)$ is large in ω compared to ρ^0
- Measurement of $A_{UT}\sin(\varphi - \varphi_s)$ in exclusive ω and ρ^0 meson will help to separate E^u and E^d

GPD Results [18]

Collab.	Year	Ref.	Observables	Kinematics			No. of points	
				x_B	Q^2 [GeV^2]	$\|t\|$ [GeV^2]	total	indep.
HERMES	2001	[4]	$A_{\rm LU}^{\sin\phi}$	0.11	2.6	0.27	1	1
CLAS	2001	[6]	$A_{\rm LU}^{\sin\phi}$	0.19	1.25	0.19	1	1
CLAS	2006	[9]	$A_{\rm UL}^{\sin\phi}$	0.2–0.4	1.82	0.15–0.44	6	3
HERMES	2006	[10]	$A_{\rm C}^{\cos\phi}$	0.08–0.12	2.0–3.7	0.03–0.42	4	4
Hall A	2006	[11]	$\sigma(\phi)$, $\Delta\sigma(\phi)$	0.36	1.5–2.3	0.17–0.33	4×24+12×24	4×24+12×24
CLAS	2007	[14]	$A_{\rm LU}(\phi)$	0.11–0.58	1.0–4.8	0.09–1.8	62×12	62×12
HERMES	2008	[15]	$A_{\rm C}^{\cos(0,1)\phi}$, $A_{\rm UT,DVCS}^{\sin(\phi-\phi_S)}$, $A_{\rm UT,I}^{\sin(\phi-\phi_S)\cos(0,1)\phi}$, $A_{\rm UT,I}^{\cos(\phi-\phi_S)\sin\phi}$	0.03–0.35	1–10	<0.7	*12*+12+12 12+12 *12*	*4*+4+4 4+4 *4*
CLAS	2008	[17]	$A_{\rm LU}(\phi)$	0.12–0.48	1.0–2.8	0.1–0.8	66	33
HERMES	2009	[19]	$A_{\rm LU,I}^{\sin(1,2)\phi}$, $A_{\rm LU,DVCS}^{\sin\phi}$, $A_{\rm C}^{\cos(0,1,2,3)\phi}$	0.05–0.24	1.2–5.75	<0.7	18+18+18 18+18+*18*+*18*	6+6+6 6+6+*6*+*6*
HERMES	2010	[21]	$A_{\rm UL}^{\sin(1,2,3)\phi}$, $A_{\rm LL}^{\cos(0,1,2)\phi}$	0.03–0.35	1–10	<0.7	12+12+*12* 12+*12*+12	4+4+*4* 4+*4*+4
HERMES	2011	[22]	$A_{\rm LT,I}^{\cos(\phi-\phi_S)\cos(0,1,2)\phi}$, $A_{\rm LT,I}^{\sin(\phi-\phi_S)\sin(1,2)\phi}$, $A_{\rm LT,BH+DVCS}^{\cos(\phi-\phi_S)\cos(0,1)\phi}$, $A_{\rm LT,BH+DVCS}^{\sin(\phi-\phi_S)\sin\phi}$	0.03–0.35	1–10	<0.7	*12*+*12*+*12* *12*+*12* *12*+12 12	*4*+*4*+*4* *4*+*4* *4*+4 4
HERMES	2012	[23]	$A_{\rm LU,I}^{\sin(1,2)\phi}$, $A_{\rm LU,DVCS}^{\sin\phi}$, $A_{\rm C}^{\cos(0,1,2,3)\phi}$	0.03–0.35	1–10	<0.7	18+*18*+*18* 18+18+*18*+*18*	6+*6*+*6* 6+6+*6*+*6*
CLAS	2015	[24]	$A_{LU}(\phi)$, $A_{UL}(\phi)$, $A_{LL}(\phi)$	0.17–0.47	1.3–3.5	0.1–1.4	166+166+166	166+166+166
CLAS	2015	[25]	$\sigma(\phi)$, $\Delta\sigma(\phi)$	0.1–0.58	1–4.6	0.09–0.52	2640+2640	2640+2640
Hall A	2015	[26]	$\sigma(\phi)$, $\Delta\sigma(\phi)$	0.33–0.40	1.5–2.6	0.17–0.37	480+600	240+360

GPD H → Transverse Charge Radius of Proton [15]

- Experimental data: DVCS at CLASS ep→epγ
- Kinematics: 0 < -t < 0.5 , 1.1 < Q2 < 2.8 and 0.067 < ξ < 0.27
- Compton Form Factor is defined as: H_{Im} (ξ, t) ≡ H^q(x, ξ, t) − H^q(−x, ξ, t).
- Fourier transform + some (small) model-dependent factor → x dependence of the proton's transverse extent

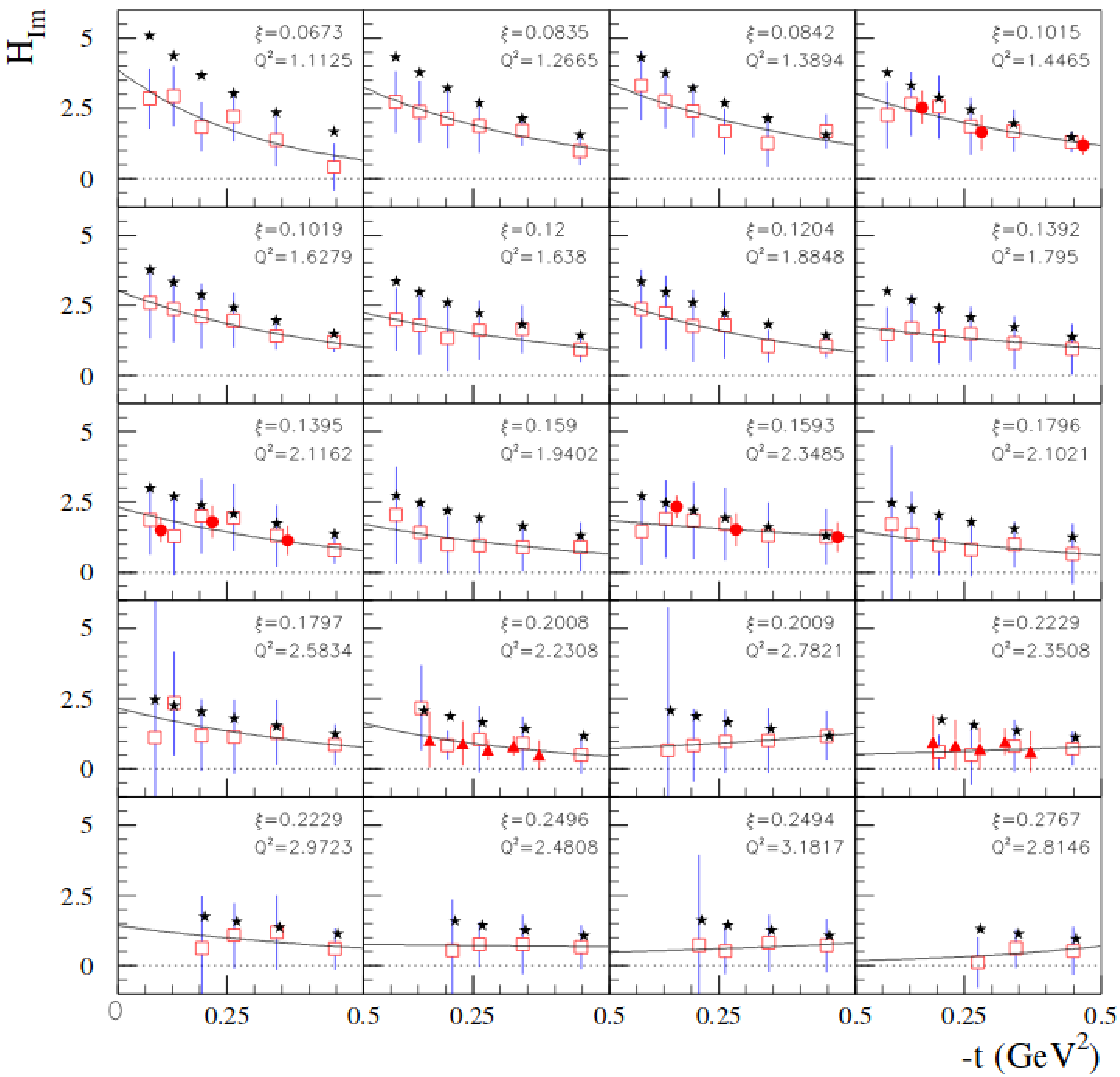

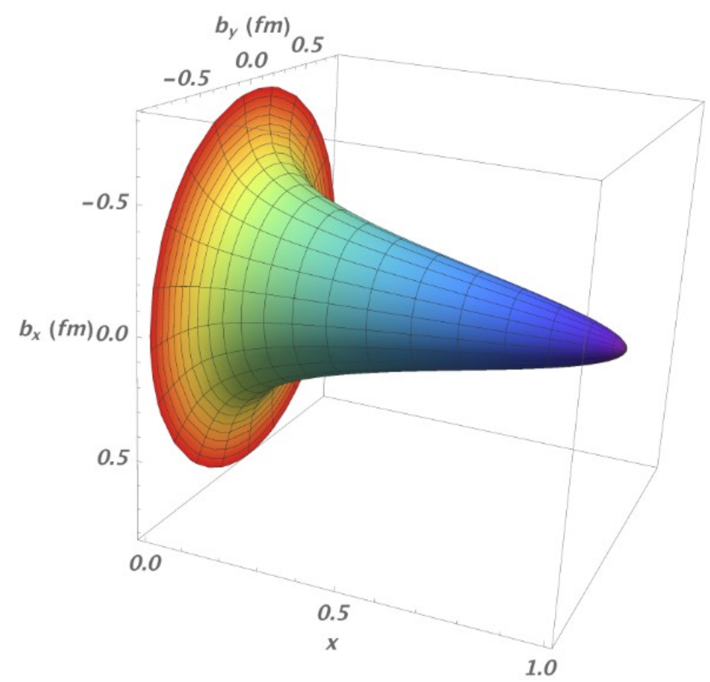

DEMP at SoLID

- Event Generator
- SoLID
- Kinematics and acceptance of DEMP at SoLID
- Proposed results

Event Generator

- Parametrization of $\boldsymbol{d\sigma_{uu}}$
- VR model[19] is used for parametrization
- A comparison of last six points of table v of[12]. Experimental data are shown in blue circles, the VR model is shown in red triangles, and our parametrization is shown in black boxes

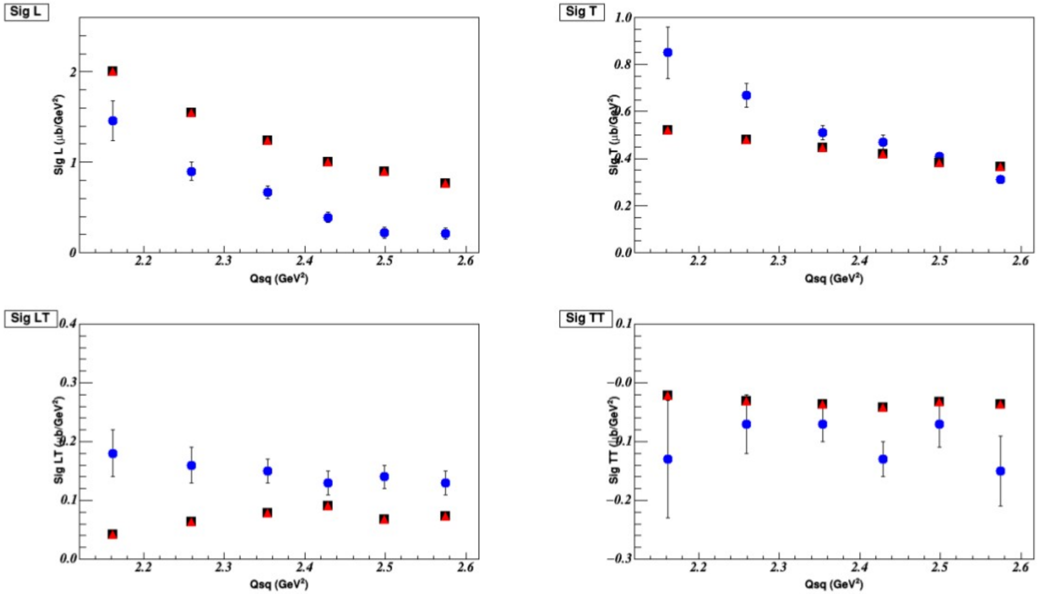

$$d\sigma_{UU} = \frac{d\sigma_{\mathrm{T}}}{dt} + \epsilon \frac{d\sigma_{\mathrm{L}}}{dt} + \epsilon \cos 2\phi \frac{d\sigma_{\mathrm{TT}}}{dt} + \sqrt{2\epsilon(\epsilon+1)} \cos\phi \frac{d\sigma_{\mathrm{LT}}}{dt}$$

$$\sigma_L = \exp\{(P_1(Q^2) + |t| * P_1'(Q^2))\} + \exp\{(P_2(Q^2) + |t| * P_2'(Q^2))\}$$

$$\sigma_T = \frac{\exp\{(P_1(Q^2) + |t| * P_1'(Q^2))\}}{P_1(|t|)}$$

$$\sigma_{LT} = P_5(t(Q^2))$$

$$\sigma_{TT} = P_5(t(Q^2))$$

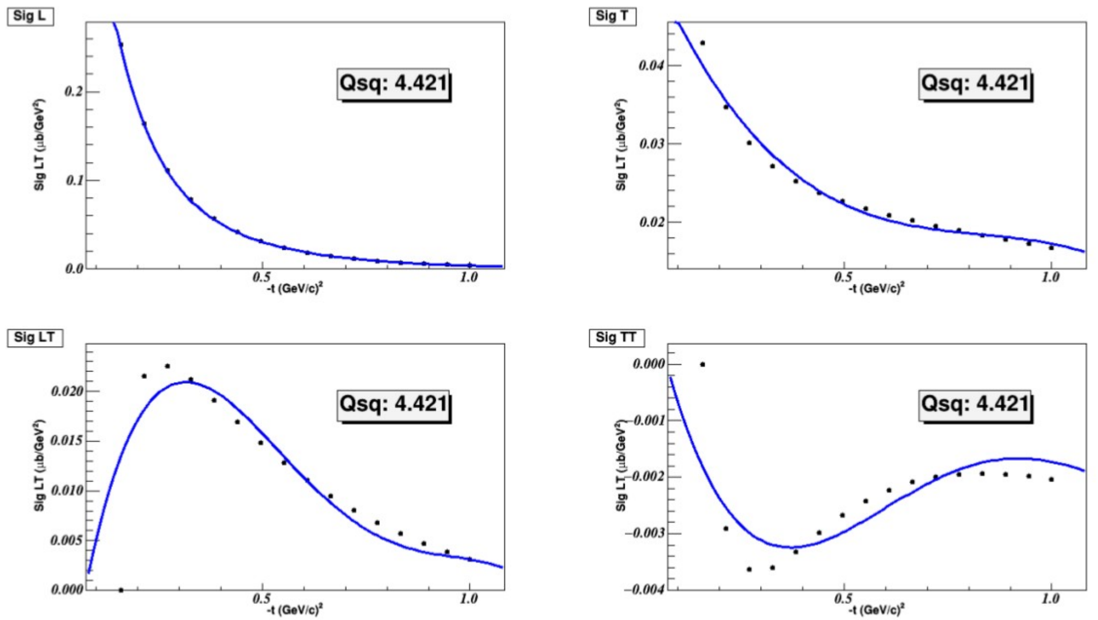

Event Generator

- Parametrization of $\boldsymbol{d\sigma_{uT}}$
- Thanks to S.V. Goloskokov, P. Kroll who provided the five asymmetries values for DEMP-SoLID kinematics.
- Rory parametrized the asymmetries

$$A_{UT}^{\sin(\mu\phi+\lambda\phi_s)_k} = \begin{cases} ae^{bx} - (a+c)e^{dx} + c, & k=1 \\ ae^{bx} + c, & k=2,3,4,5 \end{cases}$$

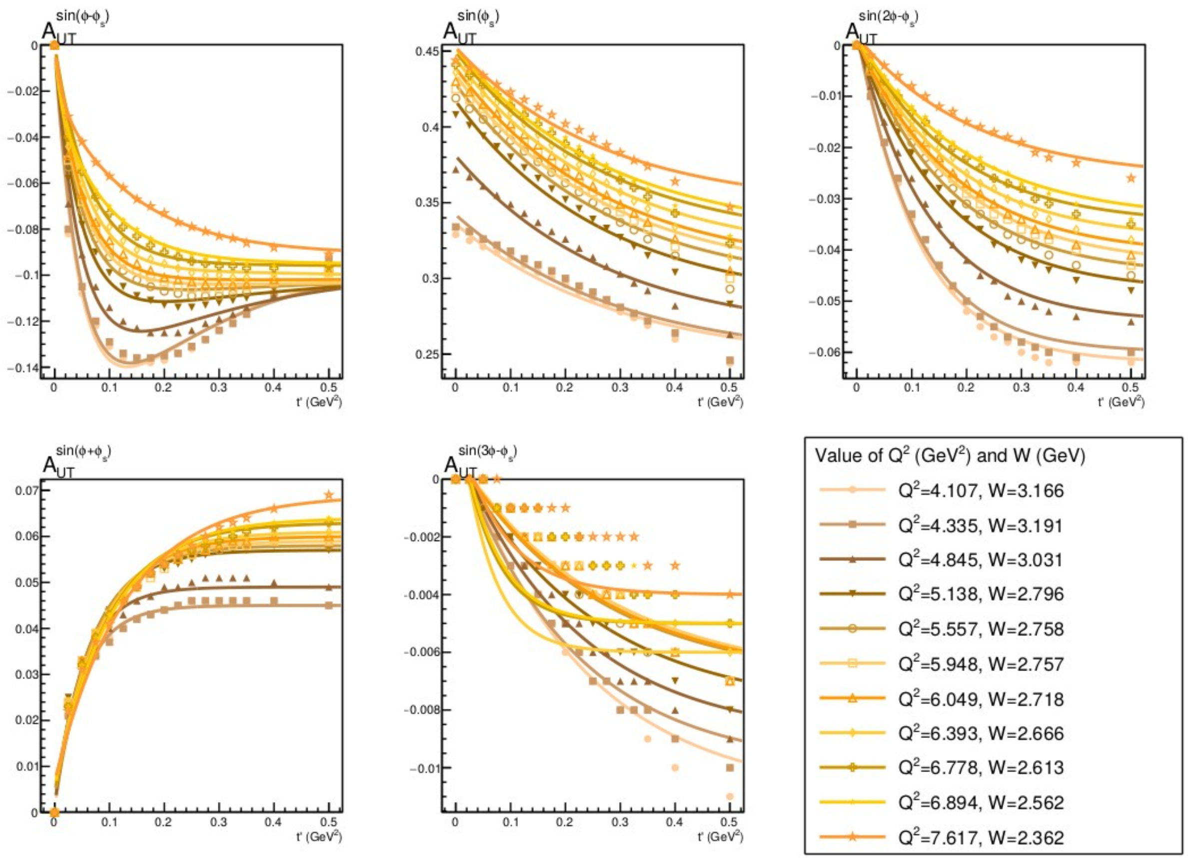

SoLID Polarized ^{3}He SIDIS Configuration

$\vec{n}(e,e'\pi^-)p$ with transversely polarized ^{3}He

- Proton is tagged, but we do not assume the momentum information is very useful.

$$\langle A_{UT} \rangle = \frac{1}{P \cdot \eta_n \cdot d} \left(\frac{N^{\uparrow} - N^{\downarrow}}{N^{\uparrow} + N^{\downarrow}} \right)$$

Run in parallel with E12-10-006:
E_0 = 11.0 GeV (48 days)
Luminosity = 10^{36} $cm^{-2}s^{-1}$ (per nucleon)

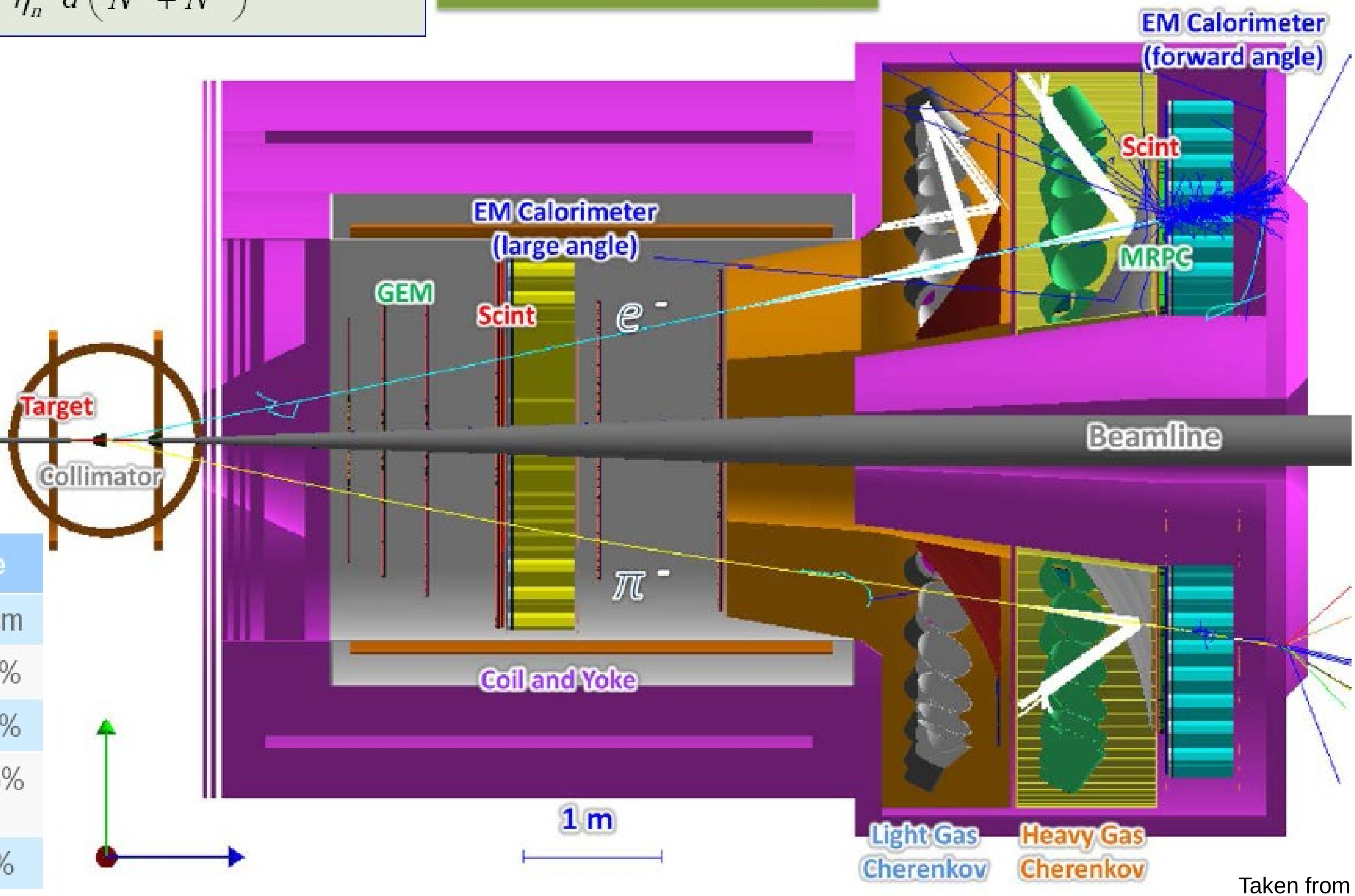

Target	^{3}He
Length	40 cm
Polarization	~60%
Dilution	~90%
Effective Neutron	86.5%
Uncertainty	~3%

Taken from [14]

SoLID

Large-Angle :
- Detect electrons and protons

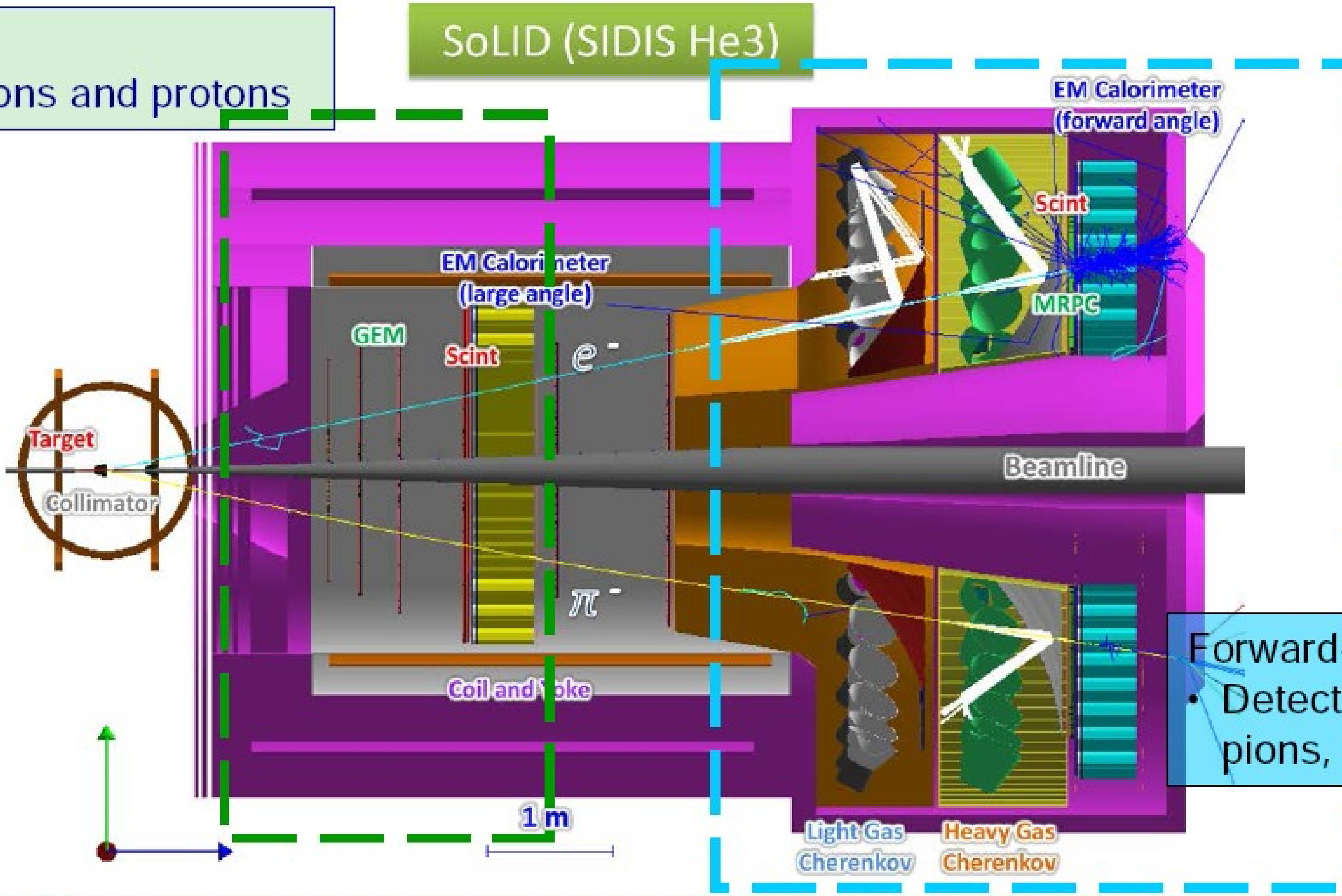

Forward-Angle :
- Detect electrons, pions, protons

$e/\pi^{\pm}$ Coverage: → Forward-Angle: $0<\varphi<2\pi$, $8^o<\theta<14.8^o$, $1<P<7$ GeV/c for $e/\pi^{\pm}$
→ Large-Angle: $0<\varphi<2\pi$, $16^o<\theta<24^o$, $3.5<P<7$ GeV/c for e only

Proton Coverage: → Same as $e/\pi^{\pm}$ at FA and LA

Resolution: $\delta P/P$~2%, $\delta\theta$~0.6 mrad, $\delta\varphi$~5 mrad

Coincidence Trigger: Electron Trigger + Hadron Trigger (pions)
Offline Analysis: Identify (tag) protons and form triple-coincidence

Recoil Particle Detection: Time of Flight

$$^{3}He(e, e'\pi^{-} p)\, pp_{sp}$$

- Need >5σ timing resolution to identify protons from other charged particles

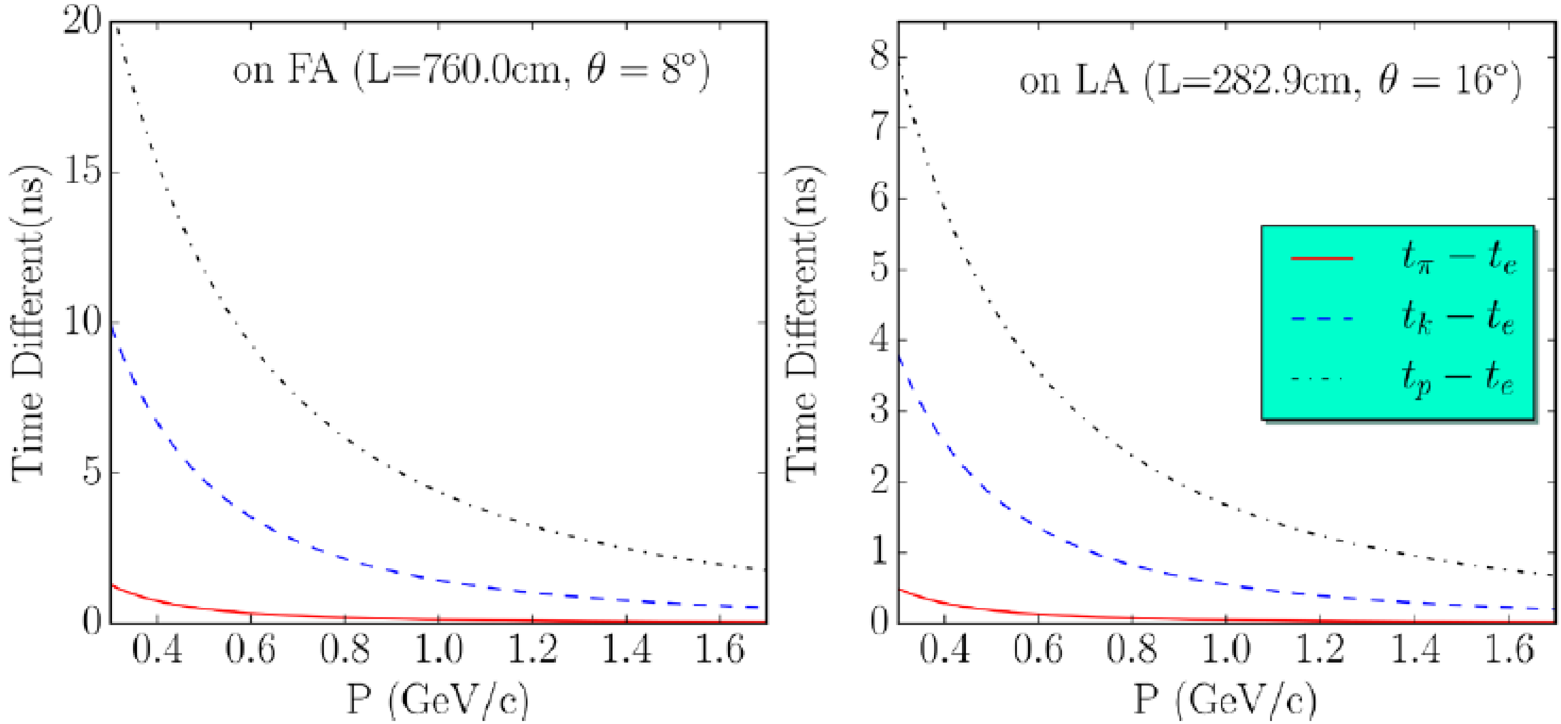

- **Exisiting SoLID Timing Detectors:**
  - MRPC & FASPC at Forward-Angle: cover 8º~14.8º, >3 ns separation.
  - LASPD at Large-Angle: cover 14º~24º, >1 ns separation.
- The currently designed timing resolution is sufficient for proton identification using TOF.

Acceptance and Projected Rates

Q^2>1 GeV^2 W>2 GeV	Q^2>4 GeV^2 W>2 GeV
DEMP: $n(e,e'\pi^- p)$ Triple Coin (Hz)	
4.95	0.40
SIDIS: $n(e,e'\pi^-)X$ Double Coin (Hz)	
1425	35.8

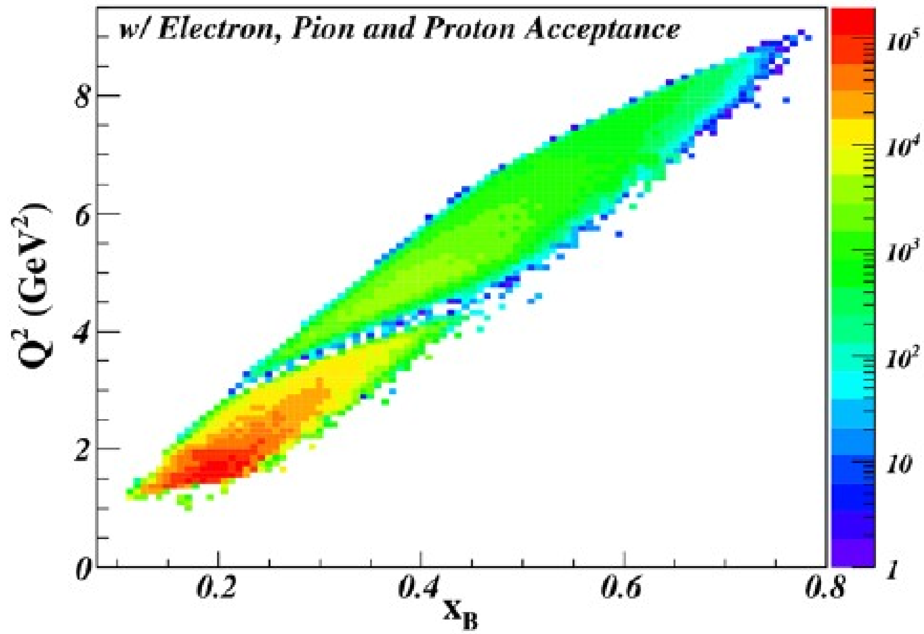

- Event generator is based on data from HERMES, Halls B,C with VR Regge+DIS model used as a constraint in unmeasured regions.
- Generator includes electron radiation, multiple scattering and ionization energy loss.
- Every detected particle is smeared in (P,θ,φ) with resolution from SoLID tracking studies, and acceptance profiles from SoLID-SIDIS GEMC study applied.

Q^2>4 GeV^2, W>2 GeV, 0.55<ε<0.75 cuts applied.

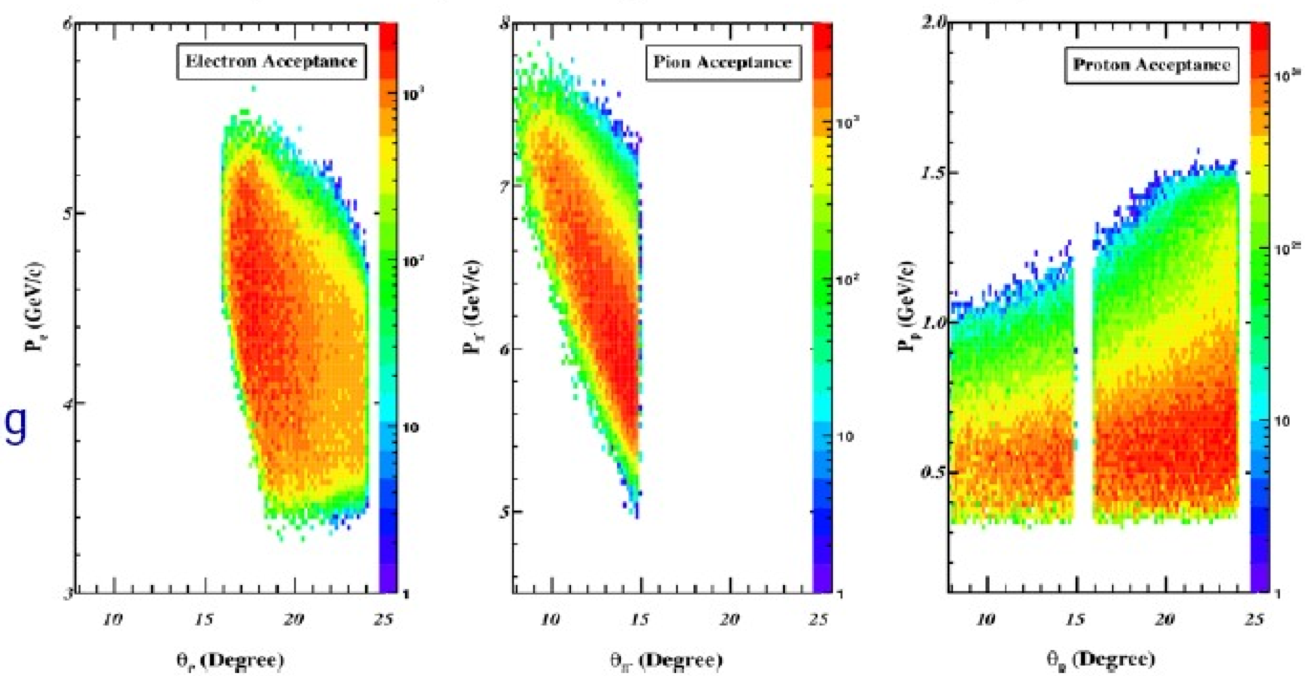

Background

Two different background channels were simulated:

- SoLID-SIDIS generator $p(e,e'\pi^-)X$ and $n(e,e'\pi^-)X$, where we assume all X fragments contain a proton (over-estimate).
- $en\rightarrow\pi^-\Delta^+\rightarrow\pi^-\pi^0p$ where the Δ^+ (polarized) decays with $l=1$, $m=0$ angular distribution (more realistic).

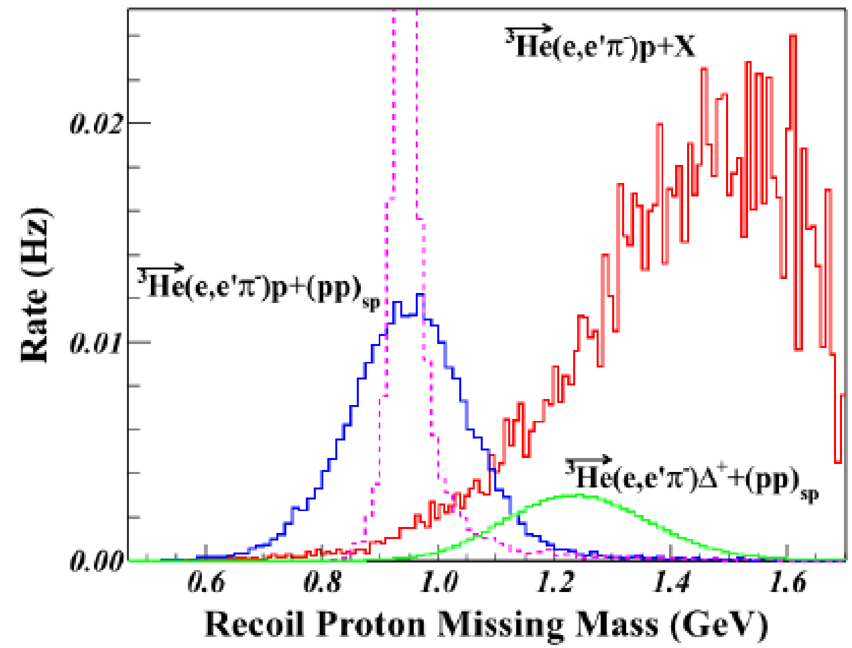

Apply P_{miss}>1.2 GeV/c cut

Scattering & radiation but no resolution smearing

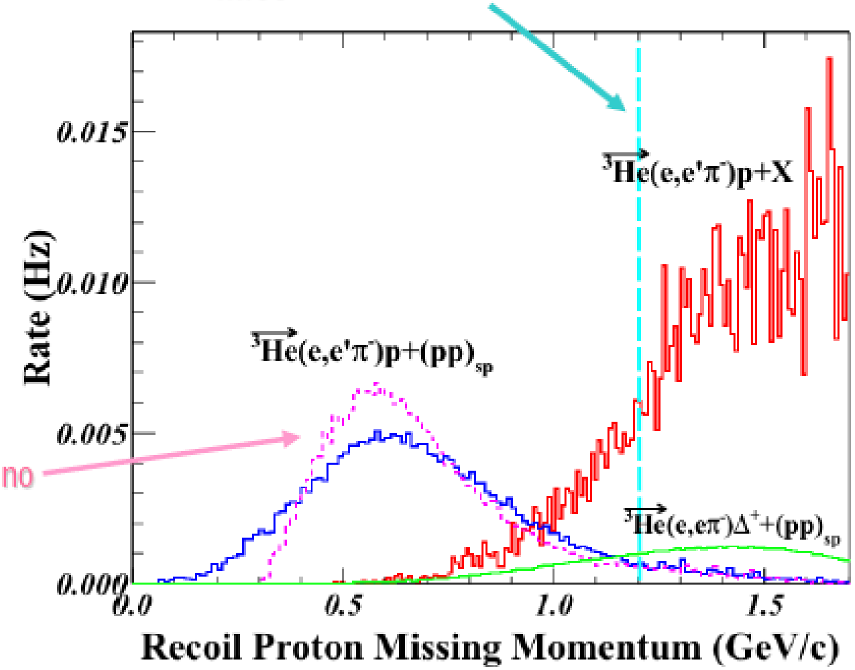

Background remaining after P_{miss} cut

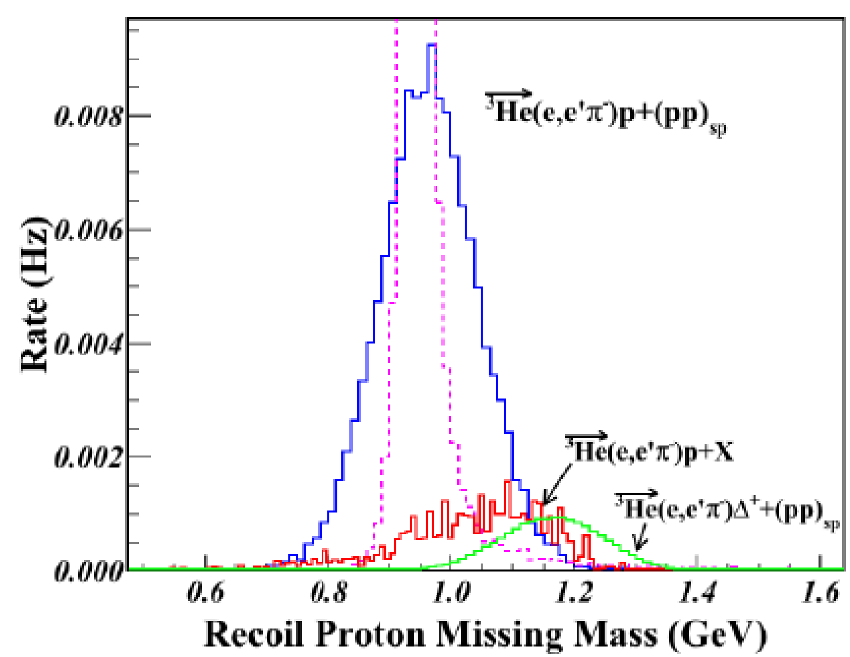

DEMP Kinematics and Bins

- **For this proposal, we binned the data in 7 *t*-bins.**
- **In actual data analysis, we will consider alternate binning.**
- All JLab data cover a range of Q^2, x_{Bj} values.
  - x_{Bj} fixes the skewness (ξ).
  - Q^2 and x_{Bj} are correlated. In fact, we have an almost linear dependence of Q^2 on x_{Bj}.
- HERMES and COMPASS experiments are restricted kinematically to very small skewness (ξ<0.1).
- **With SoLID, we can measure the skewness dependence of the relevant GPDs over a fairly large range of ξ.**

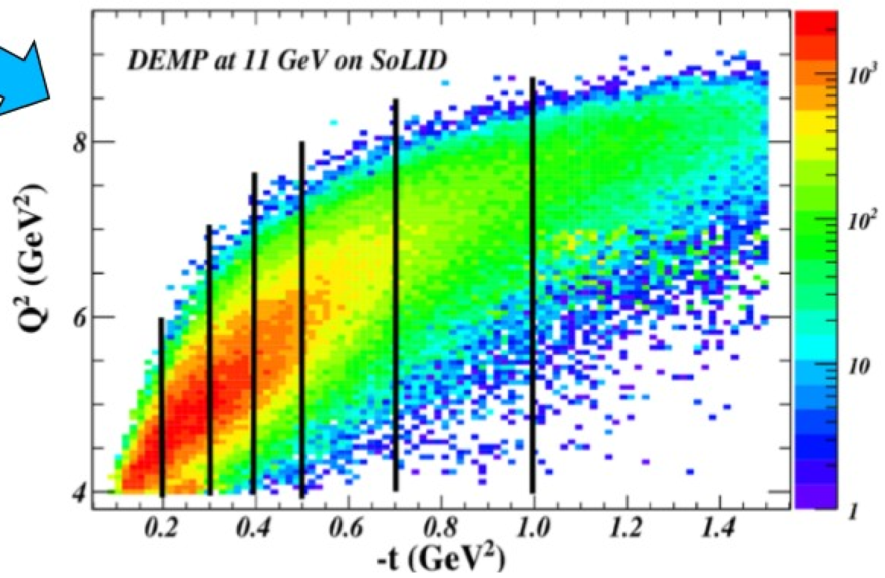

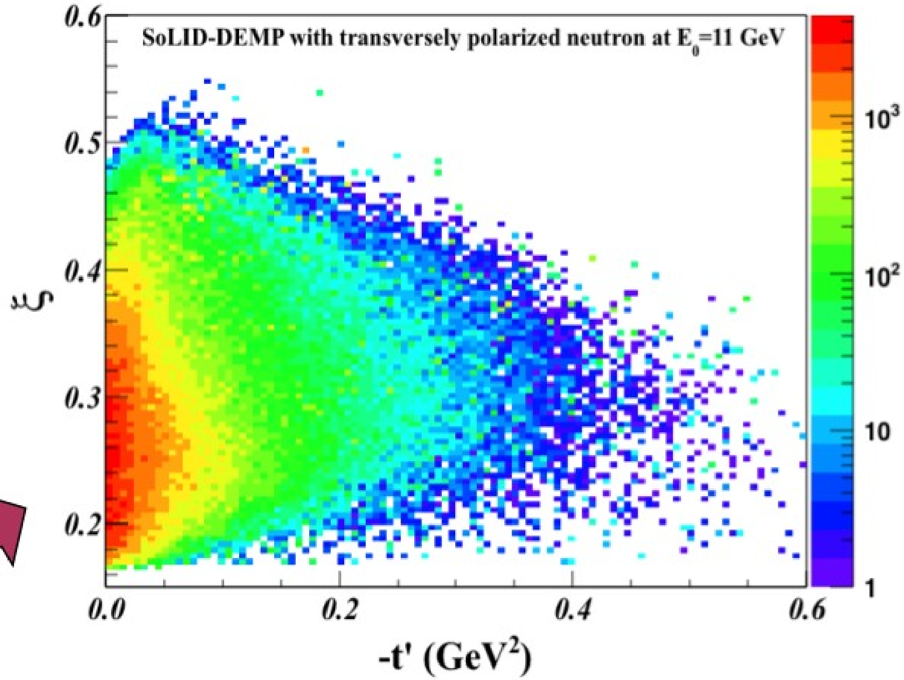

Extracting the Asymmetries

- **Same method used by HERMES in their DEMP analysis** [PLB **682**(2010)345].
- Instead of dividing the data into (φ,φ_s) bins to extract the asymmetry moments, UML takes advantage of full statistics of the data, obtains much better results when statistics are limited.

1. Construct probability density function

$$f_{\uparrow\downarrow}(\phi,\phi_s;A_k)=\frac{1}{C_{\uparrow\downarrow}}\left(1\pm\frac{|P_T|}{\sqrt{1-\sin^2(\theta_q)\sin^2(\phi_s)}}\times\sum_{k=1}^{5}A_k\sin(\mu\phi+\lambda\phi_s)\right)$$

where A_k are the asymmetries that can minimize the likelihood function.

2. Minimize negative log-likelihood function:

$$-\ln L(A_k)=-\ln L_{\uparrow}(A_k)-\ln L_{\downarrow}(A_k)$$

$$=\sum_{l=1}^{N_{MC}^{\uparrow}}\left[w_l^{\uparrow}\cdot\ln f_{\uparrow}(\phi_l,\phi_{s,l};A_k)\right]-\sum_{m=1}^{N_{MC}^{\downarrow}}\left[w_m^{\downarrow}\cdot f_{\downarrow}(\phi_m,\phi_{s,m};A_k)\right]$$

where w_l, w_m are MC event weights based on cross section & acceptance.

3. As an illustration, reconstruct azimuthal modulations & compare:

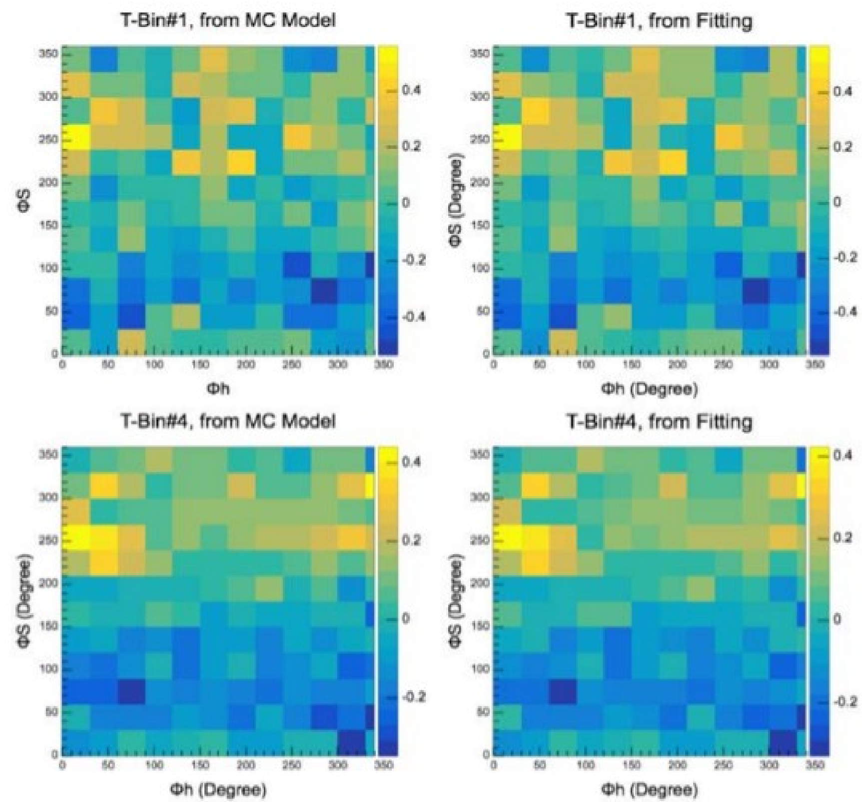

Proposed Results

All effects on.

Includes all scattering, energy loss, resolution and Fermi momentum effects.

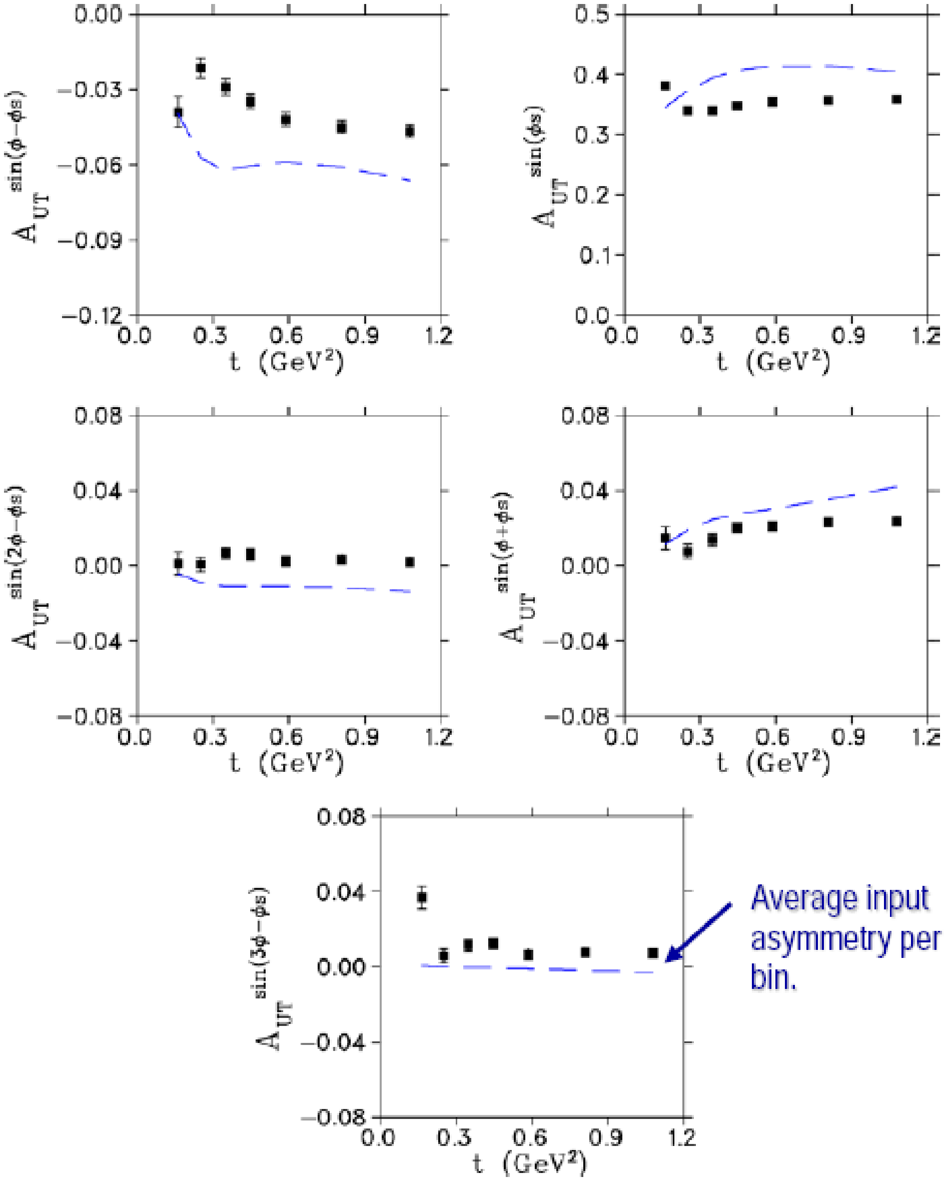

Only Fermi momentum off.

Includes all scattering, energy loss, resolution effects. Similar to where proton resolution is good enough to correct for Fermi momentum effects.

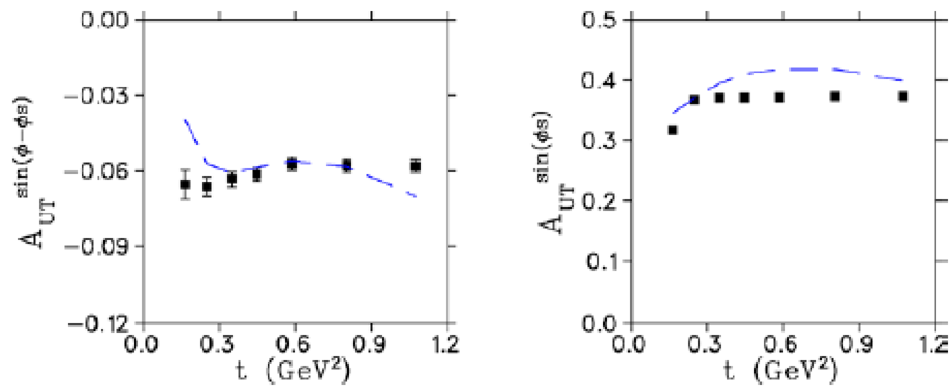

All effects off.

- Agreement between input and output fit values is very good. Validates the UML procedure.

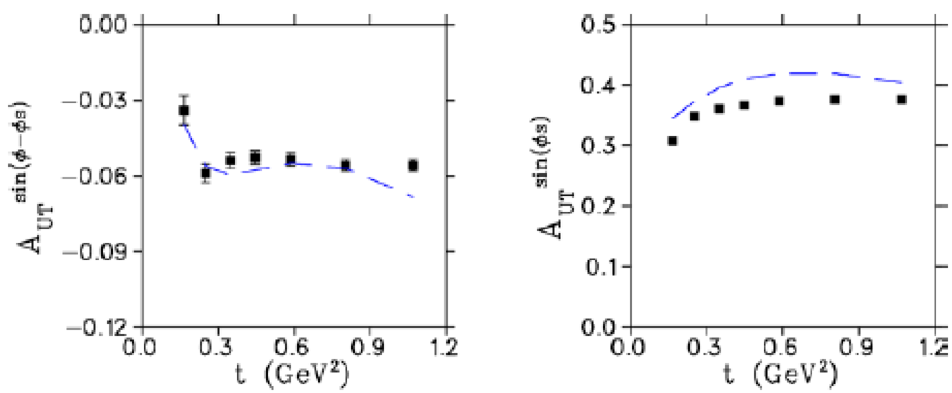

Acceptance Effects vs. (φ, φ_s)

- Expected yield as function of φ, φ_s for *t*-bins:
  - #1 (0.05-0.20)
  - #4 (0.40-0.50)
- Acceptance fairly uniform in φ_s.
- Some drop off on edges of φ distribution, since *q* is not aligned with the solenoid axis.
  - Critical feature is that φ drop off is same for target pol. up, down.

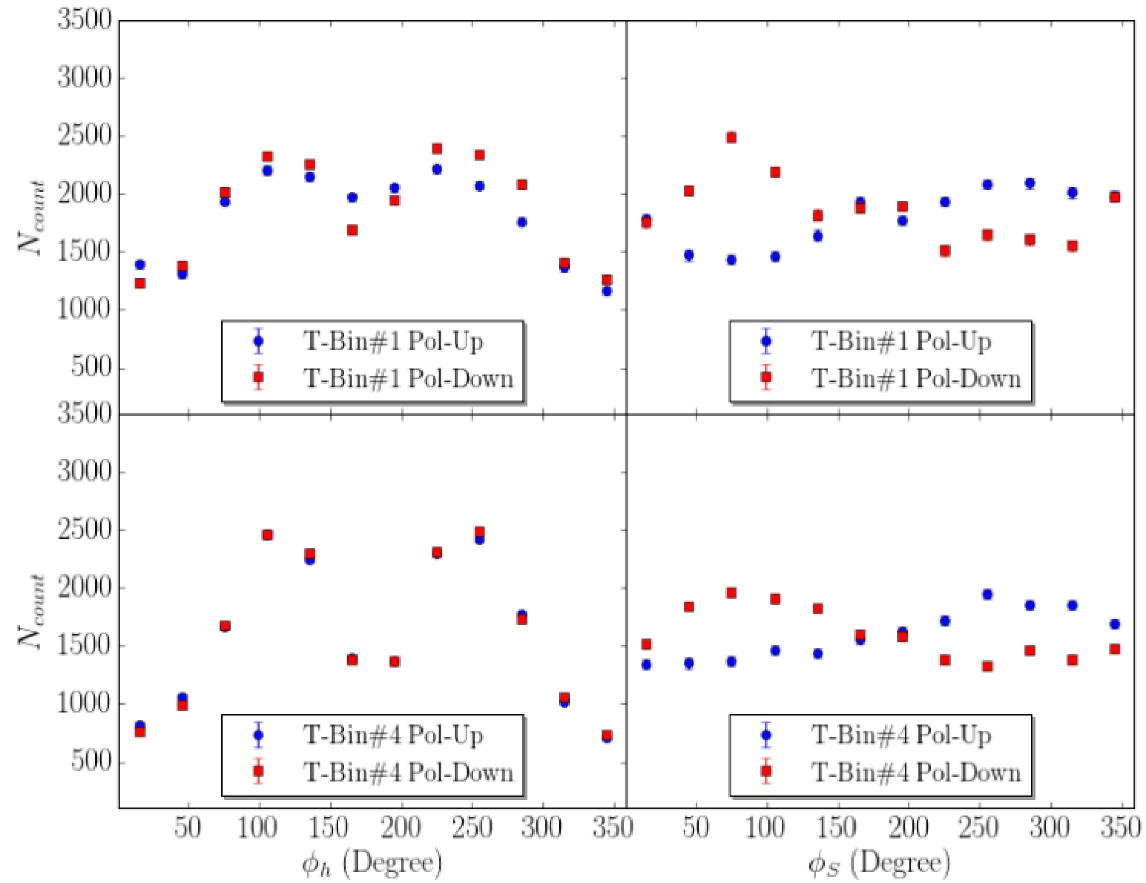

- **UML analysis shows that sufficient statistics are obtained over full (φ,φ_s) plane to extract asymmetry moments with small errors.**

HERMES data. Fig 8.4 of [6]

Bin	$<Q^2>$	$<x_B>$	$A_{UT}^{sin(\phi-\phi_S)}$	$\delta A_{UT}^{sin(\phi-\phi_S)}$	$A_{UT}^{sin(\phi_S)}$	$\delta A_{UT}^{sin(\phi_S)}$
1	1.29	0.071	0.25	0.27	0.06	0.35
2	2.02	0.109	0.00	0.24	0.54	0.29
3	4.20	0.205	0.47	0.30	1.26	0.36

Proposed Results

Bin	$<Q^2>$	$<x_B>$	$A_{UT}^{sin(\phi-\phi_S)}$	$\delta A_{UT}^{sin(\phi-\phi_S)}$	$A_{UT}^{sin(\phi_S)}$	$\delta A_{UT}^{sin(\phi_S)}$
1	4.378	0.3368	-0.0390	0.0060	0.3817	0.0059
2	4.843	0.3886	-0.0214	0.0038	0.3399	0.0038
3	5.301	0.4332	-0.0289	0.0031	0.3403	0.0031
4	5.770	0.4711	-0.0347	0.0028	0.3484	0.0028
5	6.324	0.5140	-0.0419	0.0026	0.3543	0.0025
6	6.856	0.5595	-0.0449	0.0025	0.3570	0.0024
7	7.002	0.5844	-0.0466	0.0025	0.3585	0.0024

Future Plans Phase 2
DEMP at SoLID with Recoil Detector

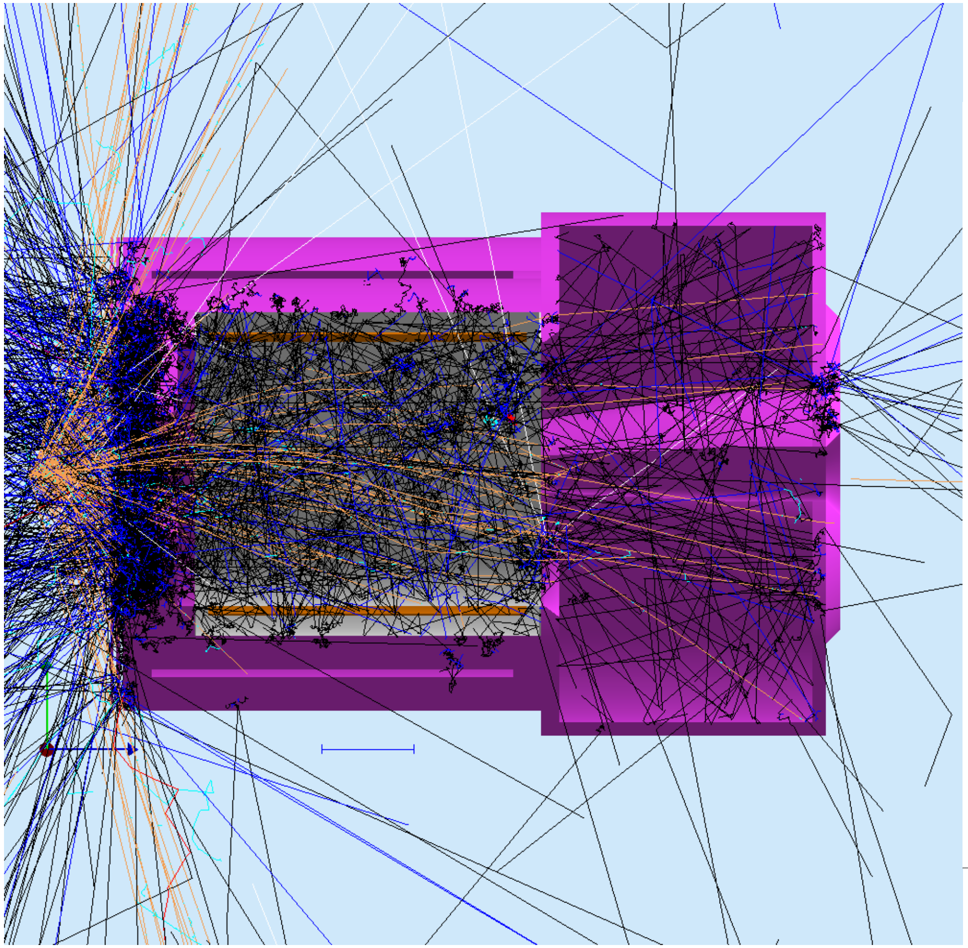

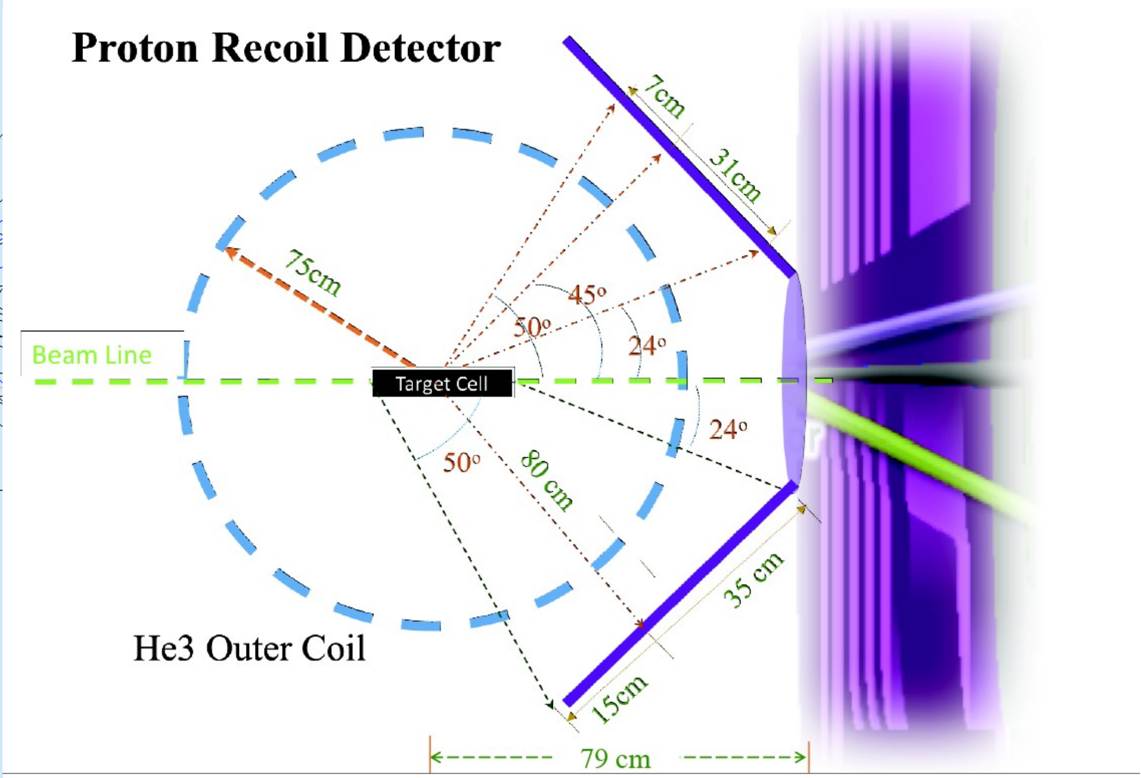

DEMP at EIC

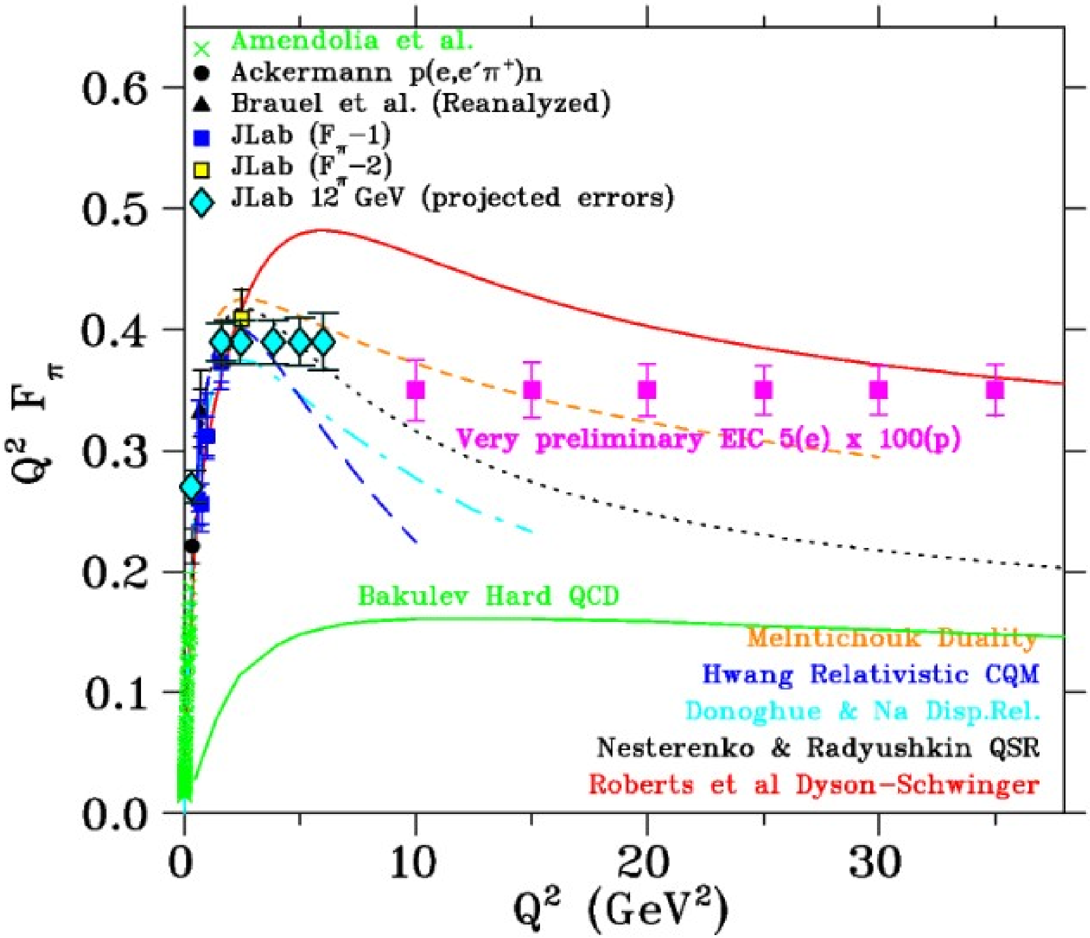

Assumptions:

- $5(e^-) \times 100(p)$.
- Integrated L=20 fb^{-1}/yr.
- Identification of exclusive $p(e,e'\pi^+n)$ events.
- 10% exp. syst. unc.
- $R=\sigma_L/\sigma_T$ from VR model, and π pole dominance at small $-t$ confirmed in ^2H π^-/π^+ ratios.
- 100% syst. unc. in model subtraction to isolate σ_L.

Much more study needed to confirm assumptions.

Summary

- $A_{UT}^{\sin(\varphi-\varphi_s)}$ transverse single-spin asymmetry in exclusive π production is particularly sensitive to the spin-flip GPD .
- $A_{UT}^{\sin(\varphi_s)}$ asymmetry can also be extracted from same data, providing powerful additional GPD-model constraints and insight into the role of transverse photon contributions at small –t, and over wide range of ξ.
- High luminosity and good acceptance capabilities of SoLID make it well-suited for this measurement. It is the only feasible manner to access the wide –t range needed to fully understand the asymmetries.
- We propose to analyze the E12-10-006 event files off-line to look for e-π--ptriple coincidence events.
- We used a sophisticated UML analysis to extract the asymmetries from simulated data in a realistic manner, just as was used in the pioneering HERMES data. The projected data are expected to be a considerable advance over HERMES in kinematic coverage and statistical precision.
- SoLID measurement is also important preparatory work for future EIC.

References

[1] Alessandro Bacchetta. Ph.D thesis.

[2] Michel Garcon. arXiv:1405.2817 [hep-ph]

[3] M. Burkardt, Phys. Rev. D 62, 071503

[4] Sigfrido Boffi, Barbara Pasquini. arXiv:0711.2625 [hep-ph]

[5] K. Goeke, M.V. Polyakov, M. Vanderhaeghen. arXiv:hep-ph/0106012

[6] Frau Magister Ivana Hristova. Ph.D. Thesis.

[7] S.V. Goloskokov, P. Kroll. arXiv:0906.0460 [hep-ph]

[8] Peter Kroll. arXiv:1611.01623 [hep-ph]

[9] M. Diehl. arXiv:hep-ph/0307382

[10] Peter Kroll. arXiv:1303.6433 [hep-ph]

[11] Peter Kroll. Eur. Phys. J. C 65, 137

[12] H.P. Blok et al. (Jefferson Lab Collaboration), Phys. Rev. C78,045202 (2008)

[13] A. Airapetian et al. (HERMES Collaboration), arXiv:0907.2596[hep-ex]

[14] SoLID Collaboration Run Group Review, June 29, 2017

[15] arXiv:1606.07821v1 [hep-ph]

[16] arXiv:1606.03725 [hep-ex]

[17] arXiv:1207.4301 [hep-ex]

[18] arXiv:1602.02763 [hep-ph]

[19] Tom Vrancx, Jan Ryckebusch. arXiv:1310.7715 [nucl-th]

[29] Nucl. Phys. B. Sup. Proc. 222-224, 187